SCIENCE CHINA
Information Sciences

December 2019, Vol. 62 220403:1–220403:24
https://doi.org/10.1007/s11432-019-2676-x

• REVIEW •
Special Focus on Two-Dimensional Materials and Device Applications

All-carbon hybrids for high-performance electronics, optoelectronics and energy storage

Shuchao QIN[1,2*], Yuanda LIU[3], Hongzhu JIANG[1], Yongbing XU[1], Yi SHI[1], Rong ZHANG[1] & Fengqiu WANG[1*]

[1]*School of Electronic Science and Engineering, Nanjing University, Nanjing* 210093*, China;*
[2]*Key Laboratory of Optical Communication Science and Technology of Shandong Province, School of Physical Science and Information Engineering, Liaocheng University, Liaocheng* 252059*, China;*
[3]*Division of Physics and Applied Physics, School of Physical and Mathematical Sciences, Nanyang Technological University, Singapore* 637371*, Singapore*

Received 26 August 2019/Revised 6 October 2019/Accepted 14 October 2019/Published online 11 November 2019

Abstract The family of carbon allotropes such as carbon nanotubes (CNTs) and graphene, with their rich chemical and physical characteristics, has attracted intense attentions in the field of nanotechnology and enabled a number of disruptive devices and applications in electronics, optoelectronics and energy storage. Just as no individual 2D (two-dimensional) material can meet all technological requirements of various applications, combining carbon materials of different dimensionality into a hybrid form is a promising strategy to optimize properties and to build novel devices operating with new principles. In particular, the direct synthesis of 2D or 3D (three-dimensional) sp^2-hybridized all-carbon hybrids based on merging CNTs and graphene affords a great promise for future electronic, optoelectronic and energy storages. Here, we review the progress of all-carbon hybrids-based devices, covering material preparation, fabrication techniques as well as applied devices. Recent progress about large-scale synthesis and assembly techniques is highlighted, and with many intrinsic advantages, the all-carbon strategy opens up a highly promising approach to obtain high-performance integrated circuits. Moreover, this review will discuss the remaining challenges in the field and provide perspectives on future applications.

Keywords all-carbon hybrids, electronics, optoelectronics, energy storage, graphene, carbon nanotube

Citation Qin S C, Liu Y D, Jiang H Z, et al. All-carbon hybrids for high-performance electronics, optoelectronics and energy storage. Sci China Inf Sci, 2019, 62(12): 220403, https://doi.org/10.1007/s11432-019-2676-x

1 Introduction

After the successful exfoliation of graphene in 2004 [1], the family of carbon allotropes has quickly established itself as an important material class that is not only rich in dimensionality but also in functionality. The family now includes 0D (zero-dimensional) fullerene, 1D (one-dimensional) CNT, 2D (two-dimensional) graphene and 3D (three-dimensional) graphite. Carbon has always been a fascinating element as a building block in living organisms as well as advanced devices. Among them, 1D CNT and 2D graphene have attracted significant attention as promising candidates for next-generation electronics optoelectronics and energy storages owing to their unique structural and physicochemical properties [2].

Graphene is a single carbon atomic plane that is composed of sp^2-bonded atoms with a honeycomb lattice [3]. One carbon atom is bonded with its three neighboring atoms via in-plane σ-bonds, which is responsible for their robustness [4]. The π-orbits perpendicular to the plane constitute the delocalized

* Corresponding author (email: lcqinshuchao@126.com, fwang@nju.edu.cn)

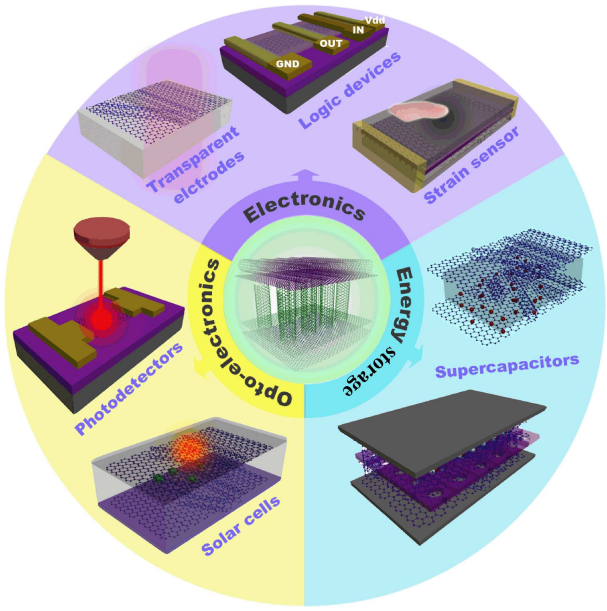

Figure 1 (Color online) Schematic of the electronic, opto-electronic devices and supercapacitors based on graphene/CNTs all-carbon materials. The main examples of the representative architecture and their main features are exhibited.

electrons network, enabling graphene a great conducting material. The conduction band and valence band of graphene contact each other at two inequivalent points of K and K' in the Fermi surface. Near Fermi surface, the bands have a linear dispersion relation, which makes the electrons and holes resemble Dirac relativistic equation (Dirac electrons) [5]. The unique electronic structure leads to the observation of fascinating physical phenomena, such as anomalous quantum Hall effect at room temperature [6] and half-integer quantization of Hall conductivity [7]. Many novel electronic [5] and photonic applications, such as transparent electrodes [8], transistors [9–11], optical modulators [12, 13], photodetectors [14–16], plasmonics devices [13, 17, 18], and ultrafast lasers, have been demonstrated [19]. The nature of zero band gap enables charge carrier generation by light absorption in a broadband range. The weak optical absorption ∼2.3% of a monolayer carbon atoms and the absence of gain mechanism, however, pose limitations on its responsivity, typically to the level of ∼10 mA/W [20]. The on/off current ratio of graphene-based transistors is ∼10, which limits its direct applicability as logic devices.

CNT is also sp^2 hybridized that could be viewed as a seamless cylinder rolled from a graphene ribbon. Their structures are specified by a pair of integers (n, m) to define their chiral vector with metallic or semiconductor characteristics [4]. Semiconducting CNT is direct bandgap, which provides a representative platform to study 1D electronics and optoelectronics. Single-CNT transistors demonstrated a high on/off ratio of $>10^5$ with a high carrier mobility ($>10^4$ $cm^2V^{-1}s^{-1}$) [21]. The packing density and drive current of single-tube transistor limit its practical application for high-performance integrated circuits [22], and individual CNT photodetectors suffer from the weak photoresponse [23]. Enhanced optical absorption can be achieved by forming CNTs thin films or networks, while their carrier mobility is severely compromised owing to accessorial scattering centers, involving surface structural damage and inter-tube contact deterioration [24–26].

In the last few years, significant efforts have been devoted for growth and post-synthetic graphene-CNTs hybrid films for high-performance electronics, optoelectronics and energy-storage. In this review, we examine the progress in synthesis of carbon nanotube, graphene and their hybrid architectures, and discuss the current state-of-the-art of the electronic optoelectronic devices and supercapacitors using all-carbon hybrids, as illustrated in Figure 1. We briefly discuss the emerging fields of study involving CNTs, graphene and their hybrids, and highlight that an all-carbon strategy is one of the most promising avenues to obtain high-performance and scalable devices. We describe the physical mechanism of electronic, optoelectronic, and energy-storage devices such as logic inverters, optoelectronic memory, electrolumi-

nescent light emitters, photodetectors and supercapacitors. Finally, we discuss the challenges facing the scalable applications and provide our perspectives on the opportunities for next-generation electronics, optoelectronics and supercapacitors technology.

2 Structures and synthesis of carbon nanotube, graphene and hybrid architectures

Carbon has a large range of allotropes in different dimensions from 0D to 3D. CNTs and graphene share the same sp^2 hybridization of carbon atoms which gives us a great opportunity to seamlessly merge 2D or 3D hybrid carbon architectures with unique physicochemical properties. To demonstrate their potential for many applications, the electronic structure and property of the carbon materials are first discussed.

2.1 Electronic structures of carbon nanotube and graphene

CNTs are best described as high aspect ratio seamless cylindrical hollow fibers, comprised of a single graphene sheet (Figure 2(a)), having diameters from one to tens of nanometers [27]. The basis vectors $a_1 = a(\sqrt{3}, 0)$ and $a_2 = a(\sqrt{3/2}, 3/2)$ generate the graphene lattice, where $a = 0.142$ nm. In cutting the graphene ribbon, a circumferential vector $C_\mathrm{h} = na_1 + ma_2$ describes its circumference, thus the nanotube radius is obtained as

$$R = \left(\sqrt{3}/2\pi\right)\sqrt{(n^2 + m^2 + nm)}. \tag{1}$$

Owing to the periodic boundary conditions of circumferential direction, rolling up a graphene sheet along different chiral vector forms either metallic or semiconducting nanotubes. For the simple orthogonal tight-binding model, the energy-momentum dispersion relation of metallic CNTs is linear near the Fermi level (E_F). Therefore, the states arbitrarily close to the Fermi level and the system is metallic. Close to E_F for semiconducting CNTs, a new dispersion relation is developed and an obvious band gap is formed at the Fermi level [28]:

$$E_g \approx \gamma_0 \frac{a}{R}. \tag{2}$$

The band gap of semiconducting CNTs is inversely proportional to its radius and approaches to zero as the diameter increasing to infinity, as shown in Figure 2(b).

The density of states (DOS) $\Delta N/\Delta E$ represent the number of available states ΔN for a given energy interval ΔE ($\Delta E \to 0$) whose shape depends on material dimensionality. For 1D CNT, the density of states shows van Hove singularities (VHSs), i.e., DOS diverges as the inverse of the square root of the energy $1/\sqrt{E}$ close to the band extrema. DOS per carbon atom can be simply expressed [29] as

$$D(E) = \frac{3a}{\pi^2 R\gamma_0} \sum_{m=1}^{N} \frac{|E|}{\sqrt{E^2 - \varepsilon_m^2}}, \tag{3}$$

where $\varepsilon_m = |3m|a\gamma_0/2R$ for metallic nanotubes and $\varepsilon_m = |3m + 1|a\gamma_0/2R$ for semiconducting nanotubes [30] showed in Figure 2(c) and (d). For metallic nanotubes, the $m = 0$ band gives a nonzero density of states at Fermi level. While for the semiconducting tubes, the DOS around 0 eV is zero.

Graphene is a planar allotrope of carbon with honeycomb lattice where all the carbon atoms form covalent bonds called σ-bonds that the $2s$ orbital interacts with the $2p_x$ and $2p_y$ orbitals to form three sp^2 hybrid orbitals in a single plane. The σ-bonds make the electrons localized along the plane and provide a well mechanical property. The unaffected $2p_z$ electrons forms delocalized π-bonds, enabling the unique electronic properties.

The rich physics of graphene, in many cases, arise from its unusual electronic structure. The valence band and conduction band of graphene meet at six points at the corner of the first Brillouin zone (see Figure 2(e)) [3]. The Fermi surface consists only of points in K-space, where DOS closes to zero,

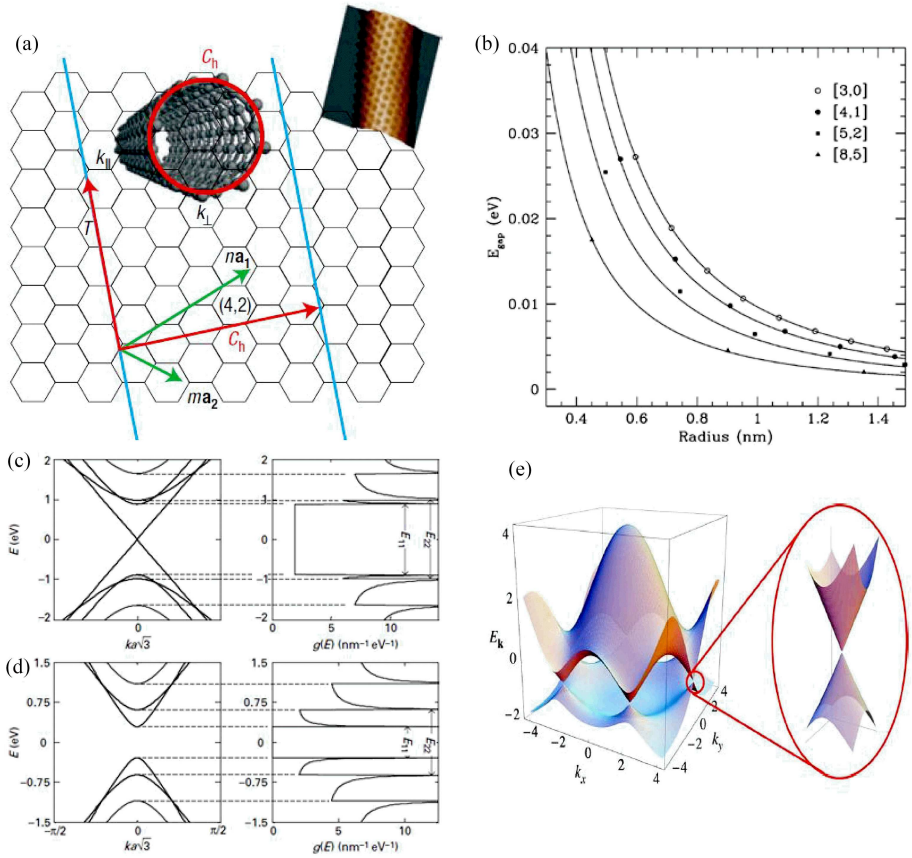

Figure 2 (Color online) The structures of carbon nanotube and graphene. (a) The carbon atoms of graphene in a honeycomb lattice. A nanotube formed by rolling a strip of graphene along the chiral vector (C_h) [4] @Copyright 2007 Macmillan Publishers Ltd. (b) Bandgaps versus nanotube radius for several selected families CNTs with different chiral [n, m] [18] @Copyright 2005 ACS. The electronic DOS for selected metallic (c) and semiconducting (d) nanotubes [30] @Copyright 2011, ACS. (e) The linear energy dispersion of graphene in the honeycomb lattice [3] @Copyright 2009 APS.

signifying that graphene is a semi-metal with zero bandgap. Close to Dirac points (Fermi points), the energy dispersion relationship can be simply expressed as a linear equation:

$$E(k) = \hbar\nu_F\,|k| = \hbar\nu_F\sqrt{k_x^2 + k_y^2}, \tag{4}$$

where k is now in spherical coordinates, $\hbar$ is the reduced Planck's constant, and $\nu_F \approx 10^6$ m/s is the Fermi velocity.

This dispersion relationship makes the electrons and holes mimic relativistic particles, because referred to as Dirac Fermionsparticles with zero effective mass. The linear DOS of graphene for low energies is mathematically expressed as

$$D(E) = \frac{2}{\pi(\hbar\nu_F)^2}\,|E| = \beta\,|E|\,, \tag{5}$$

where $\beta \approx 1.5\times10^6$ eV$^{-2}\mu$m^{-2} is a material constant, and the absolute value of E is necessary, because energy can be either positive (electrons) or negative (holes), the DOS is thus always a positive value or zero. Graphene is thus a semiconductor with zero DOS at Fermi level ($E_F = 0$).

2.2 Synthesis of carbon nanotube, graphene and all-carbon hybrids

The remarkable physical properties of CNT and graphene, such as ultrahigh carrier mobility and broadband optical absorption, make them promising candidates for next-generation electronics, photonics and optoelectronics [12, 17, 22, 31–33]. High-quality and reliable production of carbon materials is vitally

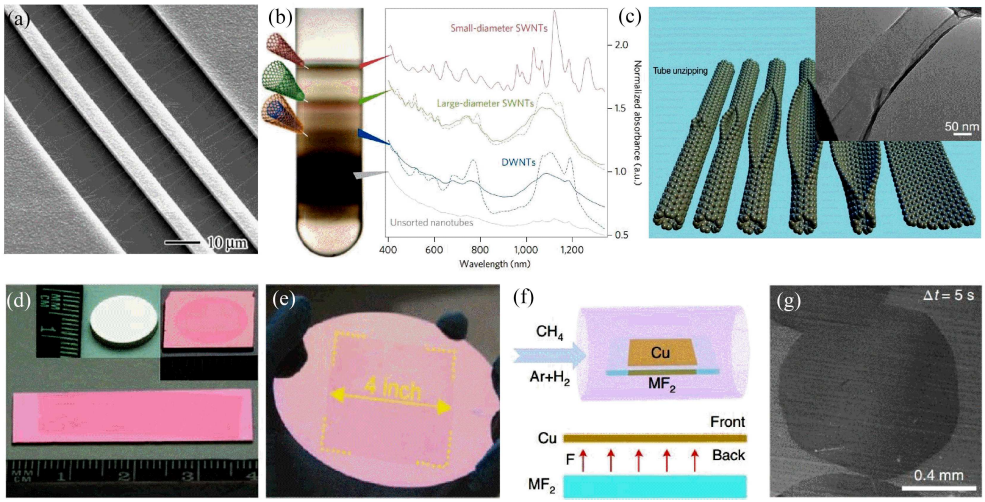

Figure 3 (Color online) Growth separation and transfer of carbon nanotubes and graphene. (a) The typical SEM image of horizontally CNTs [42] @Copyright 2001 AIP. (b) The centrifuge tube loaded with as-received nanotubes with different diameters [46] @Copyright 2009 Macmillan Publishers Ltd. (c) Unzipping diagram from a carbon nanotube to a nanoribbon. Inset: a TEM image of formed nanoribbon [54] @Copyright 2009 Macmillan Publishers Ltd. (d) Graphene transferred from the Pt foil to a SiO_2 chip [63] @Copyright 2012 Macmillan Publishers Ltd. (e) Photograph of fast growth graphene transferred on the wafer [66] @Copyright 2016 Wiley. (f) Schematics of graphene growth by local fluorine. (g) SEM image of graphene domains growing at Δt=5 s [67] @Copyright 2019 Macmillan Publishers Ltd.

important for future applications in different fields. Significant achievements in nano-carbon fabrication have been realized. In this subsection, the advantages and weaknesses of the current experimental methods for synthesizing CNT, graphene and all-carbon hybrids are reviewed.

2.2.1 *Synthesis of carbon nanotube*

Enormous efforts have been devoted for CNT synthesis, separation and purification. The synthesis of CNTs essentially requires the pyrolysis or thermal decomposition from an appropriate carbon source. Basic methods include electric arc-discharge [34–36], laser ablation [37–39], and chemical vapor deposition (CVD) [40,41]. Among them, CVD is a simple and efficient technology for large-scale synthesis. Transition metal particles are usually deposited uniformly or selectively on a substrate to form horizontally or vertically aligned nanotubes employing patterned islands strips or induced electric field (Figure 3(a)) [42]. The CNTs grown using CVD techniques have usually structural defects especially under low temperature, which seriously restricts the performance of CNTs. It is reported that the defects can be repaired by an in-situ annealing process in arc discharge and laser ablation. Furthermore, the as-produced CNTs are mixtures of metallic and semiconducting CNTs or even in form of the bundles.

In order to harvest and purify CNTs, post-treatments including dispersion, purification and separation processes are subsequently demanded. The most representative and commercially viable technique is density gradient ultracentrifugation (DGU) (Figure 3(b)), which enables separation of nanotubes with different diameter and semiconducting/metallic types [43, 44]. DGU technique also allows separation of double-walled CNTs [45, 46] and single-walled CNTs [47] employing ionic and non-ionic surfactants [48]. But the productivity and yield by using this technique are relatively low. An alternative method is gel chromatography [26]. It is able to significantly improve the chirality purity level, whereas its limitation is that it is difficult to separate large-diameter CNTs (>1.4 nm). These post-synthesis procedures above could apparently boost yield and realize the purification and separation as required but inevitably induce surface damage and inter-tube contact deterioration, which seriously limits the electron transport properties [26]. Thus selective, one-step synthesized pure metallic or semiconducting CNTs and high density array with a specific chirality on chip is of great concern at the present stage [49–51].

2.2.2 *Synthesis of graphene*

The defect-free high-quality graphene is critical for their properties and applications. Recently, graphene has been fabricated by several synthesis techniques, which can be classified: (i) top-down approach, (ii) bottom-up approach.

Owing to weak van der Waals force bonding between graphite layers, graphene can be achieved through the mechanical exfoliation technique. This technique is quite simple and economical, whereas it is impractical for large-scale practical application owing to low yield and small size. In contrast to the dry exfoliation, liquid-phase exfoliation has exhibited several advantages in terms of quantity, yield and cost, which offers a feasible way for scalability without limitation from the substrate [52]. However, single-layer graphene synthesized by this process is relatively small flakes with damaged basal plane, leading to deterioration of electrical properties. In addition, the exfoliation of graphite in an ionic liquid could yield ionic liquid functionalized graphite sheets, resulting in unintended bonding of functional surface groups [53]. Unzipping of CNTs is another versatile and efficient strategy, especially for graphene nanoribbons (GNRs, see Figure 3(c)) [54–56]. GNRs with sufficiently narrow widths open an energy band gap owing to the electrons (and holes) confinement which is significant for realizing the application in semiconductor devices [57]. However, large-area graphene cannot be achieved by nanocutting of CNTs.

Wafer-scale pristine films are crucial for realistic device applications. Epitaxial growth of graphene has been realized in silicon carbide substrate via ultrahigh vacuum (UHV) annealing [58]. This approach produces a defect-free epitaxial film in a well-defined pattern, providing a chance to directly construct electronic device. The thickness of graphene is controllable by using the annealing time and temperature. But for large-scale monolayer film, it is difficult to obtain the uniform coverage [59], and graphene on the SiC is also hard to detach and transfer, which is an insurmountable obstacle for flexible electronics. CVD is an alternative bottom-up method for largescale graphene on transition metals (e.g., Co, Ni, Cu and Pt) substrates [8, 60–63]. With the optimization of technique and process, wafer-scale graphene has been repeatedly grown on polycrystalline substrates. Its thickness and crystallinity can be controlled by growth time and cooling rate. Especially graphene layers can be detached and transferred to other arbitrary substrates, as shown in Figure 3(d). Even a 30-inch-size ultra-large monolayer graphene can be transferred on a flexible substrate [64]. In addition, the reduction from graphite oxide (GO) is widely used to produce graphene [65]. This cost-effective chemical method produces highly hydrophilic graphene. GO-derived graphene has surface defects from the harsh oxidation processes sacrificing its mechanical and electrical physical properties.

Among the various fabrication techniques shown above, CVD is one of the most promising methods for the large-scale graphene films and makes them promising for electronic and photonic applications. Without a doubt, the foundation for any modern electronic technology requires the availability of industrial-scale high-quality material in the first place. Recently, wafer-scale single-crystal graphene has been successfully synthesized by employing a modified fast growth methods [66–68]. In 2016, Wang et al. [66] presented a fast growth approach for inch-sized graphene on the single-crystalline Cu foils via oxygen chemisorption-induced reconstruction and the maximum growth rate reaches 300 $\mu m \cdot min^{-1}$. Prolonging the growth time, wafer-sized continuous graphene film can be easily synthesized and transferred onto Si substrate, as shown in Figure 3(e). Recently, Liu et al. [67] demonstrated that fluorine can accelerate the growth of the graphene even up to a rate of $\sim$200 $\mu m s^{-1}$, as shown in Figures 3(f) and (g). The barrier of methane (CH_4) decomposition is greatly reduced through fluorine substitution, and the reaction is switched from endothermic to exothermic. The sufficient carbon precursor feeding leads to a high growth rate.

2.2.3 *Synthesis of all-carbon hybrid architectures*

Graphene is theoretically a robust sp^2-hybridized structure, whereas experimentally synthesized large-area monolayer film is usually polycrystalline with high density defects, grain boundaries and even wrinkles. Polycrystalline graphene breaks easily in transfer process, if done without the assistance of a stronger polymer protective layer such as poly (methyl methacrylate) (PMMA) [8,61,69]. The electrical properties

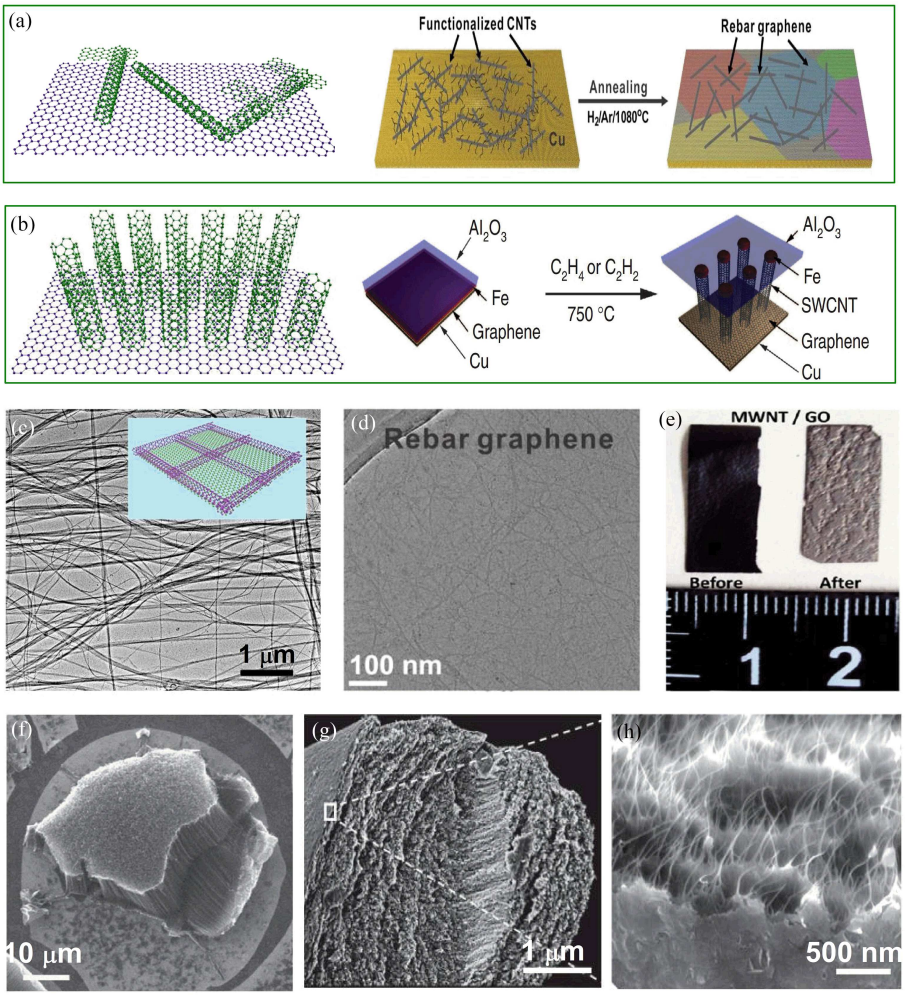

Figure 4 (Color online) Configuration models and fabrications of all-carbon hybrids. (a) Hybrids of graphene with horizontal CNTs and the typical synthesis process [77] @Copyright 2012 Macmillan Publishers Ltd. (b) Hybrids of graphene with vertical CNTs and the typical synthesis process [69] @Copyright 2014 ACS. (c) TEM and schematic of the vein-membrane-like hybrid [72] @Copyright 2013 Macmillan Publishers Ltd. (d) TEM image of interconnected SWCNT networks in rebar graphene sheets [69] @Copyright 2014 ACS. (e) Hybrid paper macroscopic appearance after thermal reduction [75] @Copyright 2013 ACS. (f) SEM of nanotube carpet [77] @Copyright 2012 Macmillan Publishers Ltd. (g) and (h) SEM images of the cross-section of all-carbon hybrid microfibers [78] @Copyright 2014 Macmillan Publishers Ltd.

of graphene degrade remarkably owing to the surface polymer contaminants. Therefore, it is significant to synthesize novel sp^2-hybridized compound, which can reinforce its in-plane mechanical strength. The covalently interconnected all-carbon hybrids may remarkably improve electronic and thermal transport properties [70, 71]. Recently, some experimental breakthroughs of graphene/CNT hybrid films have been achieved. Graphene/CNT hybrids can be mainly classified into two categories: (i) hybrids of graphene with horizontal CNTs and (ii) hybrids of graphene with vertical CNTs, as shown in Figure 4(a) and (b).

Jiang group [72] demonstrated an ultra-thin freestanding vein-membrane-like all-carbon hybrid film using the superaligned CNT arrays (Figure 4(c)). The same chemical composition and bond structure of CNT and graphene enable a strong adhesion, and the super-aligned CNT films horizontally cross-stacked upon top of graphene can serve as a porous vein-like support, which makes the hybrids to be excellent mechanical performance and electrical conductivity. Such a veinmembranelike all-carbon hybrid shows a high electron transparency close to 90%. Therefore, it can be used as gate transparency electrodes and transmission electron microscopy sample supports. However, the relatively thick graphene/CNT stacking structure causes a low optical transmittance (∼52.5% at 600 nm), which is not enough for the large-area transparent conductive electrodes. In addition, the interconnections in this physical stacking

architecture may be coupled by van der Waals' forces or π-π stacking rather than covalent bonding. Tour group has fabricated CNT-toughened graphene by annealing process and obtained robust, transparent and seamless 2D conjoined graphene/CNTs hybrids [69], which called "rebar graphene" (Figure 4(d)). In this hybrid, CNTs serve as a reinforced bar improving the film strength. Owing to the seamless covalent bonding and π-π stacking between graphene and CNTs, rebar graphene can be free-standing on water and transferred onto other substrates in a polymer-free fashion. The in-plane marriage of CNTs and graphene also improves its electrical performance. CNTs-assisted conducting pathways across grain boundaries of polycrystalline graphene sheets, providing a possibility of rebar graphene for seawater desalination [73]. Meanwhile, rebar graphene with high optical transparency can be used as flexible transparent electrodes.

In addition to the 2D hybrid film, the all-carbon quasi-3D hybrid multilayers are experimentally demonstrated. Kim group fabricated the hybrid film consisting of reduced graphene oxide (rGO) nanosheets and multiwalled CNTs (MWNTs) via layer-by-layer (LbL) assembly through the electrostatic interactions [74]. The hybrid multilayer exhibits a significantly increased conductivity after a thermal treatment with a transparency of 81% at 550 nm. However, this LbL technique requires severe chemical functionalization and has also a discount for scaleup. Terrones group fabricated paper-like all-carbon 3D hybrid films using rGO and MWNTs in aqueous dispersions assisted with cationic polyelectrolytes [75], as shown in Figure 4(e). As-fabricated hybrid films exhibit high robustness, great electronic conduction and field emission property at low voltage. The hybrid paperlike films are relatively thick and are not transparent, while they are promising in lithium-ion batteries or supercapacitors.

Another configuration to construct 3D all-carbon hybrids is by growing CNTs vertically onto graphene sheets. For this kind of graphene/CNTs hybrids, although metal catalysts (e.g., Co and Fe) are required for the vertical CNT pillars [76, 77] (see Figure 4(b)), the outstanding electrochemical properties are always retained. Tour group [77] demonstrated a high-quality 3D graphene with the vertically aligned few-walled CNT carpets seamlessly connected via covalent bonds (see Figure 4(f)). Without sacrificing their standalone properties, the Ohmic interconnected graphene-CNTs hybrids are produced with a high-surface, indicating that such a covalently bonded all-carbon hybrid material may be used in the field of energy storages. More recently, Chen group [78] demonstrated a scalable synthesis of a hierarchically structured 3D pillared all-carbon microfiber consisted of an interconnected network of aligned SWNTs (Figure 4(g) and (h)). This hybrid fiber exhibits high packing density and large ion-accessible surface and is desirable for the high-performance supercapacitors.

Graphene/CNT hybrids with different dimensionality have been proposed and successfully fabricated by various assembled methods. Different configurations own specific functional properties that make them well suited for different practical applications. A great potential application of CVD-derived graphene/CNTs hybrid films is flexible transparent conducting electrodes that typically require high optical transmittance and high flexibility simultaneously. While if one intends for energy storage applications, 3D large-area graphene/CNTs hybrids might be a better choice owing to their light weight, high mechanical strength and inert under ambient conditions.

3 All-carbon hybrids for electronics

The highly delocalized electronic structure of sp^2 hybridized carbon suggests their utility as high mobility material. Graphene possesses high carrier mobility owing to the suppressed intervalley backscattering [79, 80], which allows fast switching circuits [2]. However, graphene-based transistors cannot be turned completely off. The low on/off ratio seriously compromises its prospects for logic devices. Although the DOS at Dirac point is zero, graphene has a minimum conductivity of $4e^2/h$ at the Fermi level [7, 81–83], where e and h are the electric charge and Planck constant, respectively. The bandgap of graphene is opened by including quantum confinement in narrow graphene ribbons [84–86] or breaking the pseudospin symmetry of the K and K' carbon atoms [87, 88]. For graphene nanoribbons, the energy gap is inversely proportional to its ribbon width [84]. While the bandgap is too narrow (order of hundreds meV) for the gate-modulation at room temperature, that is so eliminated to CMOS-based digital electronics. On the

other hand, the lack of a band gap does not necessarily impede its potential for radio frequency (RF) electronics. In fact, graphene is an excellent candidate for the high speed RF devices owing to its unique performance [89–91]. For examples, high carrier mobility enables the large transconductance and 2D nature enables ideal choice for short gate length [2]. However, transport channel suffers from the doping of opposite charge carrier types at high bias [92,93], so the absence of strong current saturation is a clear weakness.

CNT with a tunable bandgap represents a promising channel material for field-effect transistors (FETs). 1D structure of CNTs eliminates small angle scattering for carriers, resulting only in forward and back scattering [79]. Free of dangling bonds brings about decreased carrier scattering [4], which is responsible for the high low-field mobility [94]. Moreover, the transistor based semiconducting CNT exhibits large on/off ratios (10^4–10^6) and low off-currents, which facilitates low-power digital electronics such as inverters [24, 95–98]. CNT FETs are intrinsically ambipolar (both p-type of hole conducting and n-type of electron conducting) that is utilized for switch operation [99]. It is crucial for precisely controlling the carrier type and construct carbon transistors in a complementary metal-oxide semiconductor (CMOS) architecture which is widely employed in modern silicon-based semiconductor industry. Currently, several doping strategies have been demonstrated to regulate majority carriers, such as chemical method [100–102], electrostatic coupling [103], trap-charge-induced doping [104], metal work-function-induced doping [105], ion implantation [106], and interface fixed charges [107]. Among them, chemical doping is efficient, which is important for the practical implementation. While stable controllable doping and n-type doping for CNTs remain a major challenge.

In addition, CNT film is chemically inert with fascinating mechanical and optical properties, making it a promising candidate for high performance, flexible, transparent and stretchable electronics using relatively simple and low-cost techniques. In recent years, hand-held and portable consumer electronics have penetrated many aspect of our daily life, which motivates research towards the novel elastic semiconductor materials that can be incorporated in modern flexible devices (e.g., touch screens and wearable communication devices) [108–110]. Until now, many flexible electronics based on carbon nanotubes have been demonstrated, such as transparent and flexible transistors on PET substrate [111], in which thick CNT (>200 tubes/μm, ∼20–30 nm) films serve as the source/drain/gate electrodes, while thin semiconducting network (∼14 tubes/μm) as the active channels. An extremely deformable and flexible all-CNT device on PVA substrate is recently reported [112]. The polymer substrate and insulator are responsible for a great flexibility and transparency compared with the metal oxides-based transistors. But the electrical performance of CNT-based transistor is not always consistent for different transistors, because the CNTs randomly connect the source/drain electrodes. Sun et al. [97] fabricated high-performance thin-film transistor (TFT) employing floating-catalyst CVD CNTs. And integrated circuits on flexible and transparent chips have also been demonstrated by using a gas-phase filtration and roll-to-roll transfer technique, which may pave the way for developing large-scale, low-cost and flexible electronics.

Despite significant progress in transparent bendable electronics based on individual graphene or carbon nanotubes, there are some remaining obstacles. The stretchable TFT requires an active channel with high on/off ratio, electrodes with excellent electrical conductivity and low contact resistance with the channels, both of which point to a cooperation strategy between carbon nanotubes and graphene. Very recently, graphene/CNTs hybrid materials have been proposed to improve its performance in electronic devices beyond the flexible devices [113–115].

Highly flexible, transparent and conductive films are one emerging technology for stretchable displays and electronic papers. In 2009, Yang group [113] reported a low-cost, scalable and modest-temperature solution strategy of graphene/CNTs hybrid films, in which no surfactants are required to preserve the intrinsic electronic and mechanical properties of both components. The all-carbon hybrids exhibit excellent conductivity at high optical transmittance of 86%, and hybrids show a better flexibility compared to the traditional transparent ITO rigid inorganic crystal structure (Figure 5(a)), indicative of complete compatibility with flexible substrates. This solution-based technique is moderate, low-cost scalable and compatible with the flexible substrates. However, for large scale integration, CVD all-carbon hybrid usually has better carrier mobility than that of liquid-phase exfoliation [113, 116–118]. For instance,

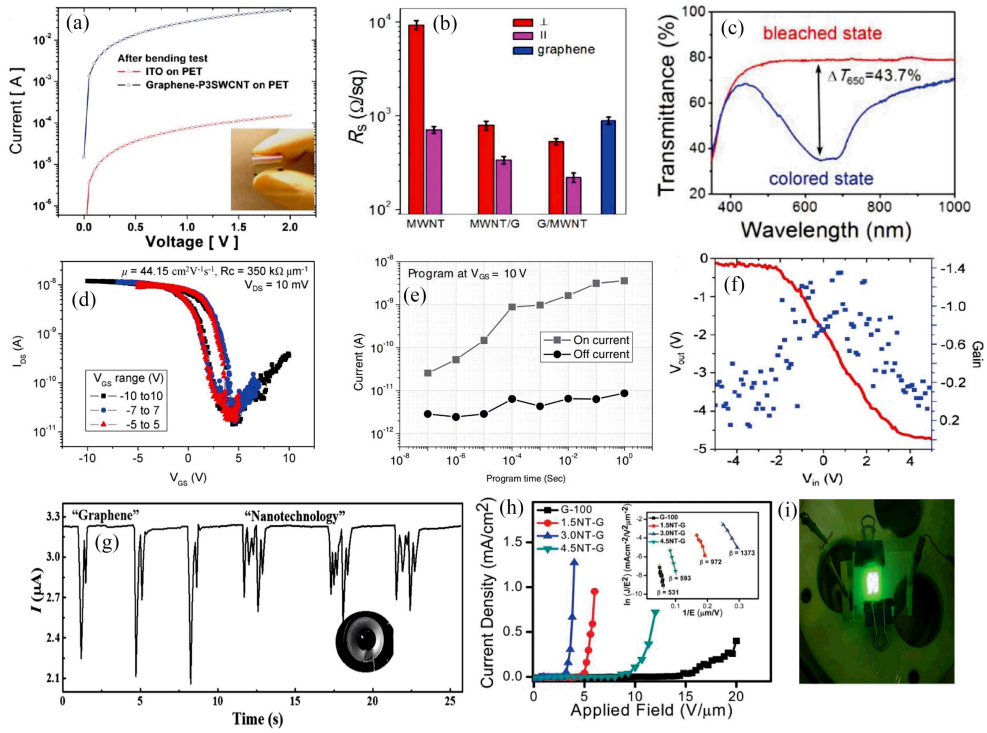

Figure 5 (Color online) All-carbon hybrids for electronic devices. (a) Transparent electrodes based on graphene/CNTs hybrid films compared with ITO films [113] @Copyright 2009 ACS. (b) The sheet resistances distribution of graphene/CNTs hybrids measured along parallel (||) and perpendicular ($\perp$) to CNT array. (c) Optical transmittance spectra of the flat electrochromic device [121] @Copyright 2015 Wiley. (d) Hysteresis of the device using graphene gate electrode [122] @Copyright 2011 ACS. (e) Current change of on/off states versus the duration time of gate pulse [123] @Copyright 2011 Wiley. (f) Output characteristics of an inverter [122] @Copyright 2011 ACS. (g) The current variations to the acoustic vibrations from different words [132] @Copyright 2017 Wiley. (h) Field emission current density as a function of applied field of graphene/CNTs hybrids with different CNT densities [137] @Copyright 2012 RSC. (i) Photograph of a field-emitting device [138] @Copyright 2010 Wiley.

the carrier mobility of rebar graphene can reach up to 200 $cm^2V^{-1}s^{-1}$, which is comparable to that of CVD polycrystalline graphene. In addition to transparent electrodes, all-carbon FETs are widely fabricated [115, 117–120]. Kholmanov et al. [121] constructed a graphene/MWNTs hybrid films by adhering a self-supporting, aligned MWNT sheet to a CVD-grown monolayer graphene. The hybrid films have the better electrical properties and exhibit anisotropic transport with the best conducting along the direction parallel to CNT alignment (Figure 5(b)). Meanwhile, the stable electrochemical feature enables such hybrid films as the excellent transparent electrodes in electrochromic devices (Figure 5(c)). Using SWNTs as the semiconducting channel and CVD graphene as a conducting electrode, Jang et al. [119] demonstrated a flexible, transparent transistor on PET substrate. The devices showed the scarcely any degradation in carrier mobility under even severe strains (∼2.2%) with a satisfactory transparency of 71.5% at 550 nm. The strong coupling between graphene and CNTs results in excellent interface contact, and the use of graphene electrodes instead of metal electrodes could dramatically reduce the hysteresis (Figure 5(d)) owing to its ideally flat and defect-free surface [122]. When some charge trap sites are introduced into the all-carbon system, a memory device can be constructed [123]. The on/off ratio is regulated by the program time, as shown in Figure 5(e). While the relatively low mobility induced by the randomly distributed CNTs array poses a serious problem which tremendously hampers its practical application for high speed electronics. Kim et al. [115] reported a simple process for controlling the orientation and density of the SWNT array through the spin coating speed. They prepared two different devices coated with horizontally aligned (type I) and longitudinally aligned (type II) SWNTs, and confirmed that the longitudinally aligned SWNTs can promote charge carriers to flow through the grain boundaries without defect scattering. A series of p-channel metal-oxide semiconductor integrated circuits (such as inverters,

NOR and NAND gates) have been realized [122]. As shown in Figure 5(f), a 0–5 V supply voltage is enough to provide the switching functions with the inverter gain of 1.4, and logic operations exhibit stable on/off state in the output terminals, indicating a potential opportunity for realistic digital circuits. Carbon materials have been attractive for wearable electronics, biomedical monitoring and motion detection owing to their unique mechanical properties. A large number of pressure sensors based on individual 1D CNTs [124–127] or 2D graphene [128–131] suffers from the problems of stability or sensitivity. Combining CNTs and graphene into hybrid materials is considered to be an effective technique to improve the pressure sensors using the synergistic effect. Jian et al. [132] assembled a flexible pressure sensor by employing aligned CNTs/graphene hybrid films. Benefiting from highly conductive hybrids with unique coalescent structure, the flexible sensor exhibits a high sensitivity, fast response speed, low detection limit and operating voltage. After carrying out more than 35000 loading-unloading cycles, it remains excellent reliability and long term stability. In particular, owing to its excellent sensitivity and operated speed, the pressure sensor can also detect acoustic signals for voice recognition (Figure 5(g)), indicative of potential great potential applications of all-carbon hybrids in smart electronics and electronic-skin.

3D all-carbon hybrids own ultralow density, high porosity, excellent electrical conductivity and robust mechanical strength and these properties promise the great potential as elastic pressure sensors. Compared with the graphene-only foam, 3D graphene/CNTs hybrids exhibit superior piezoresistive property and stability [133–135]. Improved mechanical properties and the low contact resistance of graphene and CNTs hybrids via π-π interactions have been verified [69,72,136], and effective field electron emitters are so expected in either 2D or 3D all-carbon hybrids [135,137,138]. The low turn-on and threshold electric fields have been demonstrated in 2D all-carbon hybrids (Figure 5(h)) [137]. The 3D all-carbon hybrids have been successfully integrated into a field emission device with the uniform brightness over the whole area [138], as shown in Figure 5(i). And the field emission behaviors and the enhancement factor strongly depend on the CNT density. More protruding tips (i.e., the higher CNT density) will contribute to a higher geometric field enhancement [139]. In addition to these electronic devices, all-carbon hybrids are widely used in ultralight aerogels, absorbents and gas or biosensors [135,137,140–142].

In brief, 2D CVD-grown all-carbon hybrids show clear superiority in transparent, conductive and bendable electronics, owing to their unique electrical and optical characteristics. This all-carbon construction is not applicable to logic devices, because of their gapless nature resulting from the graphene film, while other all-carbon hybrid where SWNTs is used as the semiconducting channel and graphene as a conducting electrode is a reasonable choice for transistors. In addition to electronics, another potential application area of carbon materials is photonics and optoelectronics, where the synergetic combination of various carbon allotrope's intriguing optical and unique electronic properties will be fully exploited.

4 All-carbon hybrids for optoelectronics

Graphene interacts strongly with light from infrared (IR) to ultraviolet (UV), the tunable light-graphene interaction (e.g., using an electric field or chemical dopant) allows for the construction of photodetectors and modulators. CNTs have been identified as the dream materials. In particular, semiconducting nanotubes as direct-bandgap materials are able to generate and detect photons and are of particular interest for photonics and optoelectronics. However, individual CNTs or graphene exhibit some intrinsic shortages and limitations. Graphene-based photodetectors are known to suffer from the intrinsically weak absorption characteristics and small effective photodetection areas, which limit their external quantum efficiency (EQE). Carbon nanotube exhibits either metallic or semiconductor features depending on their chiralities. Especially, semiconducting carbon nanotube exhibits excellent photoexcitations owing to 1D quantum confinement. Although extensive efforts have been made for nanotube-based photodetectors, the photoresponse of single-tube photovoltaic devices is relative weak ($<10^{-3}$ A/W) for practical application [143]. Bolometric detectors based on single-walled CNT films typically show a slow response time [144,145]. The multi-walled CNT bolometers have been also demonstrated [146], but its responsivity is limited. The major problem for individual CNT detector is that photoexcited electron-hole pairs have

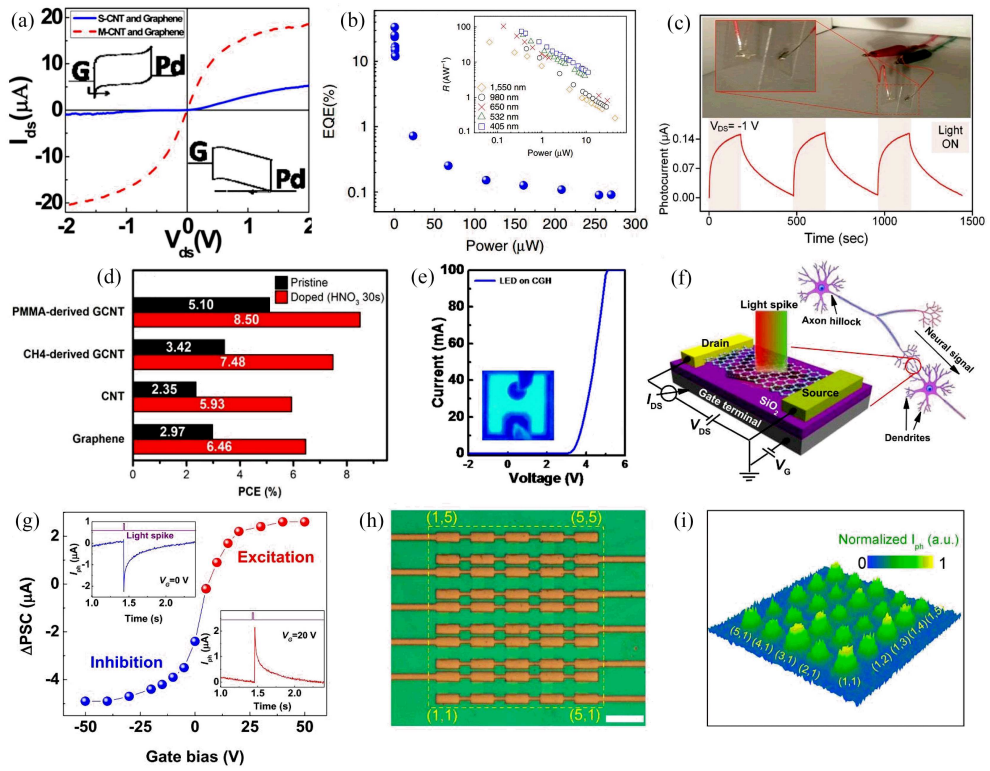

Figure 6 (Color online) All-carbon hybrids for optoelectronic devices. (a) Comparison of transport characteristics between graphene and metal CNT (m-CNT) and semiconducting CNT (s-CNT) [148] @Copyright 2011 AIP. (b) External quantum efficiency of all-carbon photodetector under 650 nm illumination. Inset shows the responsivities versus optical power of different illumination wavelengths [118] @Copyright 2015 Macmillan Publishers Ltd. (c) Images of folded photodetector and its photoresponse under a high strain of over 50% [149] Copyright 2017 Wiley. (d) Power conversion efficiency of the different solar cells [152] @Copyright 2015 IOP. (e) Electroluminescence (EL) spectra with the current in LED [157] @Copyright 2014 Macmillan Publishers Ltd. (f) Schematic illustrations of the synapse based on graphene/SWNT hybrids. (g) The change of PSC amplitudes triggered by a presynaptic light spike Insets: the typical IPSC and EPSC changes triggered by the light spike [158] @Copyright 2017 IOP. (h) Image of the integrated array based on graphene/C_{60} all-carbon hybrids. (i) The corresponding spatial-light mapping for the devices [161] @Copyright 2019 ACS.

strong binding energies [147], which exceeds the room temperature thermal energy, limiting the detector performance. The assembly of graphene/CNTs heterojunction has been proposed in virtue of their synergetic features. The intimate electronic coupling between the two sp^2-hybridized carbon allotropes is great significant for structural and chemical engineering of interfacial electronic properties which enables all-carbon heterojunctions with highly desirable charge transport. And the good contact at metallic CNT/graphene junction and obvious Schottky barrier existed at semiconducting CNT/graphene junction have been proved (Figure 6(a)) [148], which bring the new opportunities for all-carbon optoelectronics. In particular, reinforced mechanical strength and improved conductivity have been recently demonstrated by integrating a CNT network onto graphene into the all-carbon hybrids which provide exciting advantages and opportunities to produce on-chip all-carbon optoelectronic devices including photodetectors, photovoltaics, and light emitting diodes.

Photodetectors are widely used in a series of common devices in our daily life, such as remote controls and televisions. Effective separation of electron-hole pairs is crucial to obtaining high photonic response. Recently, Wang group [118] achieved a high EQE and a photoconductive gain of the photodetector by designing a planar atomically thin quasi-2D SWNT-graphene hybrids. 1D CNTs can dramatically enhance the broadband light absorption. The built-in potential at the heterostructure reduces recombination of spatially isolated photocarriers promoting effective separation of electron-hole pairs. More importantly, such an all-carbon hybrids remain the advantages of graphene and CNT, exhibiting a high electrical bandwidth of $\sim 10^4$ Hz across visible to near infrared range (inset of Figure 6(b)). The high

mobility and fast charge transfer facilitate fast temporal response. Because the charge transfer dynamics at all-carbon heterojunction is chirality-dependent [120, 148], we can develop the hybrids with controllable electrical and optical behaviors by engineering these nanoscale architectures using customized CNT chiralities. Owing to their intrinsic flexibility and the compatibility with large-scale processing, such all-carbon hybrids are the most preferred material forms for stretchable devices. Using simple assemblies processing, a transparent and flexible photodetector with remarkable photoresponse is demonstrated in all-carbon hybrids system [117], indicating the great potential of the emerging all-carbon hybrids in large-scale flexible optoelectronics. Comparing to metal/SWNT contact, the electrode contact resistance of graphene/SWNTs is as low as $\approx$0.35 M$\Omega \cdot \mu$m^{-1}, which is beneficial to efficient charge transport for high performance optoelectronic devices. A fully transparent flexible photodetector (Figure 6(c)) employing monolayer graphene and semiconducting SWNTs is constructed by Pyo et al. [149]. To enhance its photoresponsivity without sacrificing flexibility and transparency, the SWNTs network is decorated by porphyrin molecules. In addition, such all-carbon photodetector is highly sensitive to white light, can be used as an epidermal sunlight sensor for wearable healthcare devices. For IR detection, CNTs offer a promising alternative to conventional materials owing to their scalable fabrication, compatible bandgap and high absorption coefficient in IR range. The performance of CNT film-based bolometers is limited by exciton dissociation but is significantly enhanced at the graphene/CNTs interfacial heterojunctions in all-carbon hybrids [146]. All-carbon hybrids IR detector with the increased photoresponsivity compared with CNT-only IR detectors has been recently fabricated [114], demonstrating the potential toward low-cost and high-performance carbon IR detectors.

In addition to photodetectors, all-carbon hybrids are well suited for window electrodes in solar cells because of their lowcost high conductivity and chemical stability. For carbon materials, the sharp atomic edges exposed to the electrolyte and requisite defect sites can promote the catalytic reaction, and the less contact resistance between all-carbon hybrids with the electrolyte allows electrons to flow more freely which are both important for the higher power conversion efficiency. The more sharp atomic edge is created by depositing graphene flakes onto MWNTs films which promotes the reduction rate of I_3, then an dye-sensitized solar cell with excellent power conversion efficiency is built using all-carbon networks as the counter electrode [150]. In addition to 2D hybrids, utilizing 3D hybrids of graphene with vertically aligned MWNTs as the counter electrodes can also improve the accessibility with electrolyte. The dye-sensitized solar cell with satisfactory energy conversion efficiency and electrochemical properties has been reported by Choi et al. [151], employing 3D all-carbon hybrids as the counter electrodes. And the outstanding optical properties of carbon materials enable applications beyond the window electrodes in the energy conversion and storage devices. The high power conversion efficiency (8.50%) of photovoltaic device has been recorded with graphene/CNT hybrids as photoactive layer (see Figure 6(d)), in virtue of their hybridized structure [152]. The semiconducting CNTs not only facilitate the separation of carriers, but also act as the bridges to improve the overall conductance of all-carbon hybrids. And the graphene sheet guarantees an adequate and conformal contact with n-Si effectively collecting the holes generated from the photon absorption.

Very recently, graphene has been employed as a buffer layer for releasing light-emitting diodes (LEDs) or a lateral heat spreader for high power optoelectronic devices [153–155], GaN film could not be directly epitaxial grown onto graphene owing to scanty chemical reactivity. Inserting high-density ZnO nanowalls as an intermediate layer has been adopted [156], as the expense of GaN quality and operational voltage. To resolve these issues, Seo et al. [157] obtained a high-quality GaN layer employing graphene/SWCNTs hybrid structure as an intermediate layer, by reducing threading dislocation and releasing residual compressive strain (Figure 6(e)). LEDs exhibits the uniformly emitting over the whole area and even can operate well at the high injection current. All-carbon hybrid is a multi-functional photonic material, which is employed in photodetectors, LEDs and even novel neuromorphic devices. Recently, Qin et al. [158] demonstrated a photonic synapse using the graphene hybrid phototransistor, as shown in Figure 6(f). Using photonics for implementing more powerful neural networks is of increasing interest, as it may harness the superior speeds, robustness and connectivity offered by photons [159, 160]. The device can directly convert optical stimuli into electrical pulses in a highly neuron-like fashion and

exhibits flexible tuning of both the short- and long-term plasticity, as shown in Figure 6(g).

Now all-carbon hybrid based on graphene/C_{60} has attracted increasing attention because of their long-term stability, facile processing and large-scale processability [161–164] act as a potential candidate for future integrable optoelectronic applications. Wang group [161] demonstrated a large-scale integrable ultraviolet arrayed photodetector employing large-area graphene/C_{60} hybrids, as shown in Figure 6(h) and (i). Remarkably, the efficient exciton dissociation at the interface enables high photoconductive gain and a photoresponsivity exceeding 10^7 AW^{-1} for 200 nm irradiation. Interestingly, the interfacial electron-hole recombination is limited by both the carrier density in graphene and the interfacial potential barrier height, showing a gate-tunnable response time. Moreover, using the gate-tunable graphene/C_{60} interface barrier, Qin et al. [162] demonstrated an adjustable photoresponsivity of device. All-carbon hybrids have been widely used in photon detectors devices, and the efficient electronic coupling of the all-carbon hybrids and efficient exciton dissociation at the interface are the keys for high-performance detectors. In future, it can be envisioned that more all-carbon strategies will be developed for other optoelectronic functionalities involving light emission and solar harnessing applications.

Compared with individual graphene and CNT, all-carbon hybrids exhibit a series of advantages including stronger light absorption and highly efficient exciton dissociation, which increase the quantum efficiency of optoelectronic devices. Another potential application area of carbon materials is energy storage devices such as electrochemical capacitors. Compared to 2D planar structures, 3D architectures possess high active surface areas, mesoporosity and high electrolyte accessibility, which promotes the electrode-electrolyte interaction, so 3D all-carbon hybrids are more suitable to the energy storage. The implications of all-carbon hybrids for energy storage applications are discussed below.

5 All-carbon hybrids for energy storage

Recent years have witnessed growing interests in CNTs and graphene for the electrochemical energy storage applications such as supercapacitors [165–169]. High electrical conductivity and excellent charge transfer channels of CNTs make them a promising candidate for energy saving devices. While carbon nanotubes are inclined to stack in bundles, which means that only the outermost portion of CNTs function for ion absorption and the inner carbon atoms are wasted. Graphene has attracted great attention for advanced supercapacitors owing to their high surface area and outstanding mechanical strength. However, graphene electrode cannot function without a binder, which would usually decrease the specific capacitance. Recently, several routes employing graphene/CNT composite architectures, including 2D and 3D hybrids, have been proposed and successfully improved the performance of supercapacitors.

In 2009, Yu and Dai [168] fabricated a large-area and tunable 2D all-carbon hybrid film with a well-defined architecture, as shown in Figure 7(a). The resultant hybrid films exhibit a nearly rectangular cyclic voltammogram with an average specific capacitance of 120 F/g, as supercapacitor electrodes. In fact, the CNTs can act as a smart "spacer" within graphene to effectively impede the stacking, improving the accessibility for electrolyte ions [170]. CNTs can also serve as a binder to hold the graphene together, providing smoothly conductive pathways for electron conduction or hopping. Meanwhile, the graphene/CNTs hybrid architecture will provide highly porous, open channels for ion transport process, reducing the ionic diffusion length. As demonstrated by Cheng et al. [165], the graphene/CNTs composite possesses the larger current and specific capacitance, indicating that it can enhance both the energy and power performance. After 1300 cycles, the specific capacitance of CNTs declines by 9.3%, while the specific capacitance of graphene/CNTs hybrids has increased dramatically owing to electro-activation, suggesting an excellent durability. Even a longtime cycling of the graphene/CNT hybrid electrode in 1-ethyl-3-methyl imidazolium bis (trifluoromethane sulfone) imide (EMI-TFSI) can supply the power to illumine a LED (Figure 7(b)). Usually, the capacitive performance of all-carbon hybrids depends strongly on the microstructure and surface morphologies (i.e., the weight ratio of graphene/CNTs). The architectures with 9 : 1 weight ratio exhibit the highest specific capacitance of ∼326.5 F/g at 20 mV/s, which decreases with the increasing weight component of CNTs. The small amount of CNTs can effectively

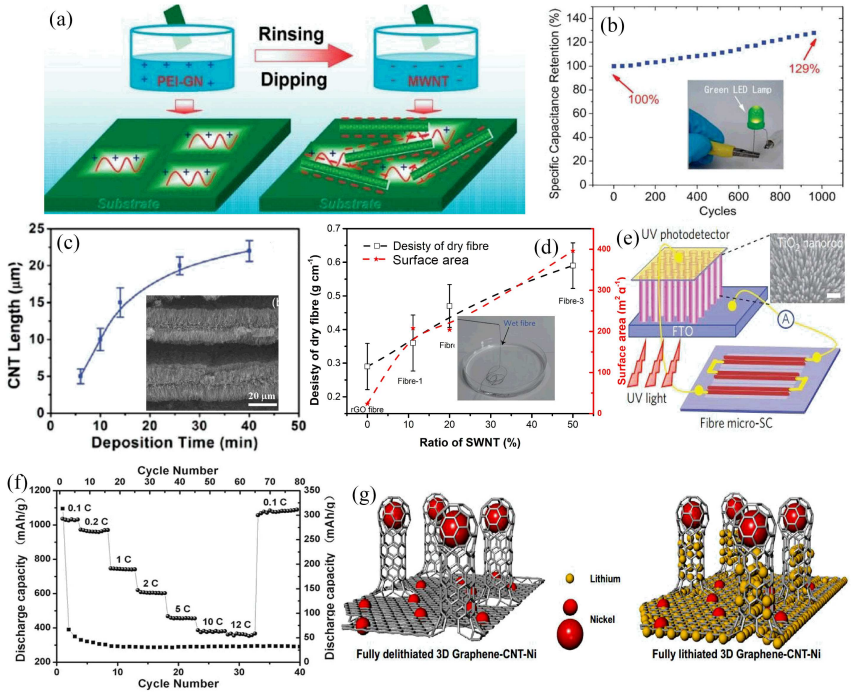

Figure 7 (Color online) All-carbon hybrids with different dimensionalities for energy storages. (a) Illustration of 2D graphene/CNTs hybrids via self-assembly process [168] @Copyright 2009 ACS. (b) Cycling performance of all-carbon composite electrode [165] @Copyright 2011 RSC. (c) Vertical CNTs pillar height versus the nanotube deposition time. Inset is a SEM image of thermally expanded graphene layers intercalated with CNTs [173] @Copyright 2011 ACS. (d) The density, surface area of hybrid fibers as a function of SWNT fraction. Inset show a photograph of the as-prepared fibers collected in water. (e) Schematic of a self-powered nanosystem. Inset: SEM of an aligned TiO_2 nanorod array [78] @Copyright 2014 Macmillan Publishers Ltd. (f) Cyclic performance and high-rate capability of the vertically aligned CNT/graphene film in a lithium-ion battery [175] @Copyright 2011 Wiley. (g) Schematics of 3D graphene/CNT-Ni nanostructure as an anode material during the charging and discharging processes in lithium-ion batteries [176] @Copyright 2013 IOP.

prevent the accumulation of graphene and enlarge its space, leading to a crumpled porous and loose architecture, while excess CNTs are ineffective for inhibiting graphene stacking. All-carbon electrodes exhibit the high-power capability, and good capability of capacitance retention, indicating that these all-carbon hybrid architectures are promising candidate materials for the next generation supercapacitors. 3D pillared architectures consisting of parallel graphene layers supported by vertically aligned CNTs possess fascinating out-of-plane electrical and mechanical properties [71,171,172]. Recently, experimental breakthrough of this novel architecture has been successfully achieved [76,166,173,174]. Using CVD method with the assistance of catalyst particles, Wei group [76] successfully obtained the first 3D CNT/graphene sandwich (CGS) structures. The aligned and short CNTs (less than 100 nm in length) are obtained under low catalyst concentration (Co: 16 wt%) with Co as carbon source, which uniformly distribute on the whole graphene sheet surface with a distance of 100–200 nm. The Brunauer-Emmett-Teller (BET) surface area of this CGS is dramatically improved (612 m^2/g, larger than that of the pristine graphene, 202 m^2/g) owing to the effective intercalation and distribution of CNTs. The incorporation of CNTs supplies additional diffusion paths, and thus facilitates rapid transport of the electrolyte ions. Therefore, CGS shows a great capacitance up to 385 F/g as well as excellent electrochemical stability. With increasing the reaction time, the increased effective interfacial area is able to enhance effective capacitance, which is significant to the practical application. Roy and co-workers have created a tunable 3D pillared all-carbon network vertically by intercalated growth of aligned CNTs into thermally expanded highly ordered pyrolytic graphite (HOPG) [173]. In brief, the acid-treated HOPG is expanded along the graphite *c*-axis using heating, then this expanded HOPG is treated in a tube furnace at high temperature in the Ar/H_2 mixture gas. Finally, the 3D pillared all-carbon architecture is produced by pyrolysis of FePc. By controlling the FePc pyrolysis time, the length of CNT pillars can be regulated, as shown in Figure 7(c). More importantly, these inherently porous all-carbon architectures can be served

as an effective scaffold of other pseudocapacitive active materials for highperformance supercapacitors. Therefore, an excellent average specific capacitance of 1384 F/g with long-term stability is obtained in this 3D all-carbon framework. However, it is noted that limited by the unstable catalyst nanoparticles (NPs), the as-grown CNTs on the graphene surface are usually mixed up with carbon nanofibers using above-mentioned methods. Compared with MWCNTs, SWNTs show higher specific surface area and lower defect density. 3D graphene/SWCNTs hybrid architecture has more superiority and attraction for advanced energy storage. Recently, one-step CVD growth of these hybrids has been realized on FeMgAl layered double hydroxides (LDHs) flakes under ∼950° [174]. Because of its large specific surface area, great structural stability and abundant porosity, the all-carbon composites exhibited excellent rate performance for Li-S batteries. As shown in the cyclic voltammogram (CV) profiles, the electrochemical characteristics of the SWCNT/graphene cathode are very stable. For the cycling stability, even at current density (up to ∼5 C), a capacity of 650 mAh·g^{-1}can still be preserved after 100 cycles. The in situ deposition of SWCNTs and graphene technique is significant to fabricate all-carbon hybrids, and makes a step forward to their realistic applications in nanocomposites and electrochemical energy storage devices.

Except these configurations, other novel all-carbon hybrids are recently assembled. Yu et al. [78] developed a scalable way to continuously produce the hierarchical SWNT/rGO fibers using a silica capillary column. The hybrid fibers have high packing density, large ion-accessible surface area and the interconnected porous structure, which are responsible for high volumetric performance supercapacitors. Adding the fraction of SWNT, the density, surface area and conductivity of hybrid fibers would increase (Figure 7(d)), and SWNT alignment could also be enhanced by the inter-tube hydrogen-bonding interaction. For 1 M H_2SO_4 in the three-electrode cell, this hierarchical structure exhibits the best specific volumetric capacitance of 305 F·cm^3, resulting from their synergistic effect. For the full micro-supercapacitor with PVA/H_3PO_4 gel electrolyte without the binder, the volumetric energy density is ∼6.3 mWh·cm^{-3}, which is much higher than that of commercially available supercapacitors. Such all-carbon hybrid supercapacitor can power a TiO_2-based ultraviolet photodetector (Figure 7(e)), and it can also be integrated into miniaturized flexible devices as an external power source. All-carbon hybrids show considerable appeal in energy conversion and storage devices. Li et al. [175] grew CNTs directly onto a freestanding graphene paper by using CVD method to construct vertically aligned CNT/graphene all-carbon hybrids. The hybrids as lithium-ion battery electrode materials show a stable discharge capacity of 290 mAh·g^{-1} at 30 mA·g^{-1} after 40 cycles, with good coulombic efficiency, high-rate capability and cycling performance, as shown in Figure 7(f). Such all-carbon hybrid can be employed as an integrated electrode combining the active component and current collector for lithium-ion battery. The reason is that all-carbon hybrids with 3D network nanostructure process an ultrahigh surface area, a large number of activation sites and efficient ion pathways, all of which are crucial for high capacity anode materials in lithium-ion batteries [176], as shown in Figure 7(g).

All-carbon hybrids with different architectures and dimensionalities exhibit different electronic properties and device performance and could be an appropriate alternative for different applications. Table 1 presents a comparison of the technical features of all-carbon hybrids for electronics, optoelectronics and energy storages. Compared with individual graphene and CNT, 2D planar all-carbon hybrids exhibit stronger light absorption and efficient exciton dissociation at their interface, which is well suited for optoelectronic devices. 3D all-carbon architectures exhibit high active surface area, abundant mesoporosity and electrolyte activation sites, which is better for energy storages. CNTs, graphene and their hybrids have attracted enormous attentions in electronics, optoelectronics and energy storage, owing to their technically superior in the mobility, optical transmittance, mechanical strength and chemical stability. Despite tremendous advancements, the practical application and industrialization are still faced with some challenges.

6 Challenges and perspectives

A significant application is the transparent and flexible electrode. For the electrodes based on CNTs film, the electrical conductivity should be further improved by solving the inter-tube contact resistance, the

Table 1 Comparison of technical features of all-carbon hybrids for electronics, optoelectronics and energy storages

Architecture	Electronics	Optoelectronics	Energy storages
Individual CNT	High carrier mobility and small on/off ratio for metallic CNTs; Larger on/off ratio and limited carrier mobility for semiconducting CNTs	Limited response time and responsivity from UV to NIR	High electrical conductivity but tends to stack into bundles
Individual graphene	High carrier mobility but small on/off ratio	Ultrafast photoresponse (GHz) but limited responsivity from UV to THz	High surface area, chemically stable but easily forms irreversible agglomerates
2D planar CNT/graphene	High carrier mobility and limited on/off ratio due to graphene	Strong light absorption and high carrier mobility; efficient exciton separation at interface; fast response time and high photoresponsivity	Well suited for optoelectronics such as photodetectors
3D vertical CNT/graphene	Well suited for energy storages such as Li-ion batteries	Strong light absorption and high carrier mobility; improved photoresponsivity	High surface-to-volume ratio; abundant mesoporosity and activation sites

dispersion and the mechanical adhesion to the substrates. Although graphene shows a great mechanical adhesion, the transfer process remains a challenge, which is often suffered from wrinkles and crack formation resulting from the grain boundaries and defects. The recently emerged hybrid systems (covalently bonding CNTs to graphene) may enhance the overall electrical and mechanical properties [69, 136, 177] and even can be allowed for polymer-free transfer process. While for high-throughput manufacturing in flexible carbon electronics, the printing techniques involving screen/gravure printing and inkjet printing will be the technical direction in the future owing to their advantages in terms of costs and production speed. All-carbon hybrids in solution that are suitable for the printing process need further exploration and optimization. Semiconductor CNT films can behave as channels in transistors, while device-to-device variability remains an issue, uniform CNT films (in purity and dispersity) with semiconducting behavior should be further improved by growth and post-separation methods. In addition, the extrinsic factors such as the effect of metal contacts, dielectric layers, underlying substrate, and surrounding environment must be managed. For graphene-based logic transistor, the deficiency of bandgap is an unbridgeable obstacle, opening a larger bandgap is desirable but remains a big challenge. A band gap can be opened in graphene through quantum confinement in narrow nanoribbons, but the mobility is severely degraded owing to the carrier scattering and charge localization when the width is less than 10 nm. Finding methods of mass production of GNRs with a ribbon width of $<$10 nm without the edge scattering will be an important technical advance. Another potential strategy is employing graphene/CNTs hybrids, in which semiconductor CNTs act as transistor channel for high on/off ratio with graphene as electrodes to guarantee high mobility. Graphene and CNT exhibit the ambipolar behavior, however, p-type transfer characteristics are usually obtained under ambient conditions owing to the adsorption of water and oxygen. Passivation of carbon nanomaterial to control electron concentration is of importance for building up CMOS, which has the two merits compared with either PMOS or NMOS devices: the larger noise immunity and the smaller static power consumption. Investigations and developments of graphene/CNTs hybrid transistors will be a promising research area for the accessible, low-cost and high-performance logic transistors and even sophisticated carbon-based integrated circuits, where CNTs and graphene lend themselves advantages through their synergistic effects. We should put more effort into this research topic in the future.

In addition to electronic devices, carbon materials exhibit a great potential in photovoltaic devices

as both the electrodes and active channels. As the channels of photodetectors, graphene suffers from weak light absorption and low photoresponsivity. The detectors based on CNTs or CNT films exhibit either low responsivity or slow response time. Design of new architecture to improve the photoresponsivity of graphene photodetectors without sacrificing operational speed is of great importance. A series of heterogeneous schemes including plasmonic resonance, evanescent-wave and conventional semiconductor coupling have been explored. However, problems remain in photoresponsivity and large-scale fabrication. Coupling CNTs with graphene can increase the light absorption, reduce recombination of spatially isolated photocarriers at the 1D-2D junction by promoting effective excition separation. All-carbon hybrid is a promising candidate material for phototransistors with balanced and tunable gain-bandwidth characteristics. The strategies available for all-carbon hybrid film can be divided into the post-fabrication and one-step-fabrication, which have different limitations and advantages for various applications. For example, the post-fabrication can be realized by simple spin-coating, and even obtain the tunable interfacial electronic properties by regulating CNTs concentrations. The one-step-fabrication graphene/CNT hybrid films can be synthesized by annealing functionalized CNTs or using a solid phase pyrolysis method. These hybrid films possess reinforced mechanical strength, and exhibit both high transparency and electrical conductivity, while these methods usually require high growth temperature and indispensable catalysts. The synthesis conditions in catalyst CVD need to be optimized for the stable and reproducible production of all-carbon hybrids. The super-aligned CNT arrays may be used in practical applications such as low-cost TFTs and logic devices. Although dense, aligned arrays of CNTs have been demonstrated through the CVD technique, the one-step-fabrication of all-carbon hybrids with horizontally aligned CNTs remains a big challenge. Additional efforts in the direction of the graphene/CNTs hybrid film are needed to further our understanding of density control of CNTs, which has an important influence on the electrical and optical properties of hybrid films.

Recently, the flourishing wearable electronics require the multifunctional energy-storage architectures that allow the fold and stretch without sacrificing their electrical functions. Carbon nanotubes, graphene and their hybrids have great potential for this purpose owing to unique physical and mechanical stability. Despite a large amount of research publications, lots of challenges are still under dispute for the practical and commercial implications. Using the porous electrodes as the flexible electrodes is suffering from their low mechanical strength during repeated deformation. Athough this value of elasticity can be improved by fabricating graphene/CNTs all-carbon hybrids, the repeated deformation still leads to some micro-cracks between electrodes and substrates. In future, high-throughput flexible manufacturing urgently calls for new preparation technologies for fabricating robust flexible electrodes, such as holographic patterning and inkjet printing.

Combining 1D CNTs and 2D graphene into planar or vertical all-carbon hybrids is considered to be a potential strategy to fabricate all-carbon devices without introducing any noncarbon impurities. At present, several main challenges remain to be unsolved for the practical applications and much more efforts are required to understand and improve their electronic, optoelectronic and mechanical properties. Developing robust all-carbon hybrids with enhanced performances by employing the low-cost, scalable and industrial production technologies is urgent. Generally, the growth CNTs are mixtures of intrinsic semiconducting and metallic nanotubes. For the transparent electrodes of all-carbon films, the metallic CNTs/graphene hybrids with good electronic performance and mechanical strength are required, while the semiconducting CNTs/graphene hybrids with dramatic absorption and efficient charge transfer are great for the photodetector and photovoltaic devices. In situ synthesis control of CNT length, diameter and chirality grown on the graphene surface to form single-chirality CNT/graphene all-carbon hybrids according our requirement will be a key research topic as well as a big challenge. In future, the action of incorporating the multifunctions into one self-powered device or non-planar multi-dimensional integration based on all-carbon materials is also an appealing trend.

7 Conclusion

In summary, the development of graphene/CNT hybrids with a number of tunable properties shows

promising applications in electronics, optoelectronics and energy storage. In the future, it is possible to revolutionize all aspects of our daily life in a self-sufficiency all-carbon structure from the power supply, different functional elements to integrated system. Investigations and developments of all-carbon hybrids will be one of the most active research areas for fabricating the high-performance individual device and even all-carbon-based integrated circuits. Nowdays, the most significant task is to exploit and fabricate large-scale, stable and tunable all-carbon hybrids by using a low-cost, high-yield, and industrial compatibility technique for various applications.

Acknowledgements This work was supported in part by National Key R & D Program of China (Grant Nos. 2018YFB22-00500, 2017YFA0206304), National Basic Research Program of China (Grant No. 2014CB921101), National Natural Science Foundation of China (Grant Nos. 61775093, 61427812), National Youth 1000-Talent Plan, 'Jiangsu Shuangchuang Team' Program, and Jiangsu NSF (Grant No. BK20170012).

References

1 Novoselov K S. Electric field effect in atomically thin carbon films. Science, 2004, 306: 666–669
2 Jariwala D, Sangwan V K, Lauhon L J, et al. Carbon nanomaterials for electronics, optoelectronics, photovoltaics, and sensing. Chem Soc Rev, 2013, 42: 2824–2860
3 Castro Neto A H, Guinea F, Peres N M R, et al. The electronic properties of graphene. Rev Mod Phys, 2009, 81: 109–162
4 Avouris P, Chen Z H, Perebeinos V. Carbon-based electronics. Nat Nanotech, 2007, 2: 605–615
5 Bonaccorso F, Sun Z, Hasan T, et al. Graphene photonics and optoelectronics. Nat Photon, 2010, 4: 611–622
6 Zhang Y, Tan Y W, Stormer H L, et al. Experimental observation of the quantum Hall effect and Berry's phase in graphene. Nature, 2005, 438: 201–204
7 Novoselov K S, Geim A K, Morozov S V, et al. Two-dimensional gas of massless Dirac fermions in graphene. Nature, 2005, 438: 197–200
8 Kim K S, Zhao Y, Jang H, et al. Large-scale pattern growth of graphene films for stretchable transparent electrodes. Nature, 2009, 457: 706–710
9 Liao L, Lin Y C, Bao M Q, et al. High-speed graphene transistors with a self-aligned nanowire gate. Nature, 2010, 467: 305–308
10 Yang H, Heo J, Park S, et al. Graphene barristor, a triode device with a gate-controlled schottky barrier. Science, 2012, 336: 1140–1143
11 Lin Y M, Valdes-Garcia A, Han S J, et al. Wafer-scale graphene integrated circuit. Science, 2011, 332: 1294–1297
12 Liu M, Yin X B, Ulin-Avila E, et al. A graphene-based broadband optical modulator. Nature, 2011, 474: 64–67
13 Ansell D, Radko I P, Han Z, et al. Hybrid graphene plasmonic waveguide modulators. Nat Commun, 2015, 6: 8846
14 Liu C H, Chang Y C, Norris T B, et al. Graphene photodetectors with ultra-broadband and high responsivity at room temperature. Nat Nanotech, 2014, 9: 273–278
15 Baugher B W H, Churchill H O H, Yang Y, et al. Optoelectronic devices based on electrically tunable p-n diodes in a monolayer dichalcogenide. Nat Nanotech, 2014, 9: 262–267
16 Pospischil A, Furchi M M, Mueller T. Solar-energy conversion and light emission in an atomic monolayer p-n diode. Nat Nanotech, 2014, 9: 257–261
17 Koppens F H L, Chang D E, Garcia de Abajo F J. Graphene plasmonics: a platform for strong light-matter interactions. Nano Lett, 2011, 11: 3370–3377
18 Low T, Avouris P. Graphene plasmonics for terahertz to mid-infrared applications. ACS Nano, 2014, 8: 1086–1101
19 Sun Z P, Hasan T, Torrisi F, et al. Graphene mode-locked ultrafast laser. ACS Nano, 2010, 4: 803–810
20 Konstantatos G, Badioli M, Gaudreau L, et al. Hybrid graphene-quantum dot phototransistors with ultrahigh gain. Nat Nanotech, 2012, 7: 363–368
21 Franklin A D, Chen Z H. Length scaling of carbon nanotube transistors. Nat Nanotech, 2010, 5: 858–862
22 Cao Q, Han S J, Tulevski G S, et al. Arrays of single-walled carbon nanotubes with full surface coverage for high-performance electronics. Nat Nanotech, 2013, 8: 180–186
23 Itkis M E, Borondics F, Yu A, et al. Bolometric infrared photoresponse of suspended single-walled carbon nanotube films. Science, 2006, 312: 413–416
24 Geier M L, Prabhumirashi P L, McMorrow J J, et al. Subnanowatt carbon nanotube complementary logic enabled by threshold voltage control. Nano Lett, 2013, 13: 4810–4814
25 Park H, Afzali A, Han S J, et al. High-density integration of carbon nanotubes via chemical self-assembly. Nat Nanotech, 2012, 7: 787–791
26 Liu H P, Nishide D, Tanaka T, et al. Large-scale single-chirality separation of single-wall carbon nanotubes by simple gel chromatography. Nat Commun, 2011, 2: 309
27 Zhu H W, Xu C L, Wu D H. Direct synthesis of long single-walled carbon nanotube strands. Science, 2002, 296: 884–886
28 Charlier J C, Blase X, Roche S. Electronic and transport properties of nanotubes. Rev Mod Phys, 2007, 79: 677–732
29 Mintmire J W, White C T. Universal density of states for carbon nanotubes. Phys Rev Lett, 1998, 81: 2506–2509

30 Wong H S P, Akinwande D. Carbon Nanotube and Graphene Device Physics. Cambridge: Cambridge University Press, 2011
31 Barone P W, Baik S, Heller D A, et al. Near-infrared optical sensors based on single-walled carbon nanotubes. Nat Mater, 2004, 4: 86–92
32 Bahk Y M, Ramakrishnan G, Choi J, et al. Plasmon enhanced terahertz emission from single layer graphene. ACS Nano, 2014, 8: 9089–9096
33 Behnam A, Sangwan V K, Zhong X Y, et al. High-field transport and thermal reliability of sorted carbon nanotube network devices. ACS Nano, 2013, 7: 482–490
34 Iijima S. Helical microtubules of graphitic carbon. Nature, 1991, 354: 56–58
35 Ebbesen T W, Ajayan P M. Large-scale synthesis of carbon nanotubes. Nature, 1992, 358: 220–222
36 Iijima S, Ichihashi T. Single-shell carbon nanotubes of 1-nm diameter. Nature, 1993, 363: 603–605
37 Thess A, Lee R, Nikolaev P, et al. Crystalline ropes of metallic carbon nanotubes. Science, 1996, 273: 483–487
38 Guo T, Nikolaev P, Rinzler A G, et al. Self-assembly of tubular fullerenes. J Phys Chem, 1995, 99: 10694–10697
39 Guo T, Nikolaev P, Thess A, et al. Catalytic growth of single-walled manotubes by laser vaporization. Chem Phys Lett, 1995, 243: 49–54
40 Li W Z, Xie S S, Qian L X, et al. Large-scale synthesis of aligned carbon nanotubes. Science, 1996, 274: 1701–1703
41 Hata K, Futaba D N, Mizuno K. Water-assisted highly efficient synthesis of impurity-free single-walled carbon nanotubes. Science, 2004, 306: 1362–1364
42 Zhang Y G, Chang A, Cao J, et al. Electric-field-directed growth of aligned single-walled carbon nanotubes. Appl Phys Lett, 2001, 79: 3155–3157
43 Arnold M S, Green A A, Hulvat J F, et al. Sorting carbon nanotubes by electronic structure using density differentiation. Nat Nanotech, 2006, 1: 60–65
44 Arnold M S, Stupp S I, Hersam M C. Enrichment of single-walled carbon nanotubes by diameter in density gradients. Nano Lett, 2005, 5: 713–718
45 Green A A, Hersam M C. Properties and application of double-walled carbon nanotubes sorted by outer-wall electronic type. ACS Nano, 2011, 5: 1459–1467
46 Green A A, Hersam M C. Processing and properties of highly enriched double-wall carbon nanotubes. Nat Nanotech, 2009, 4: 64–70
47 Green A A, Hersam M C. Nearly single-chirality single-walled carbon nanotubes produced via orthogonal iterative density gradient ultracentrifugation. Adv Mater, 2011, 23: 2185–2190
48 Antaris A L, Seo J W T, Green A A, et al. Sorting single-walled carbon nanotubes by electronic type using nonionic, biocompatible block copolymers. ACS Nano, 2010, 4: 4725–4732
49 Yang F, Wang X, Zhang D Q, et al. Chirality-specific growth of single-walled carbon nanotubes on solid alloy catalysts. Nature, 2014, 510: 522–524
50 Yang F, Wang X, Si J, et al. Water-assisted preparation of high-purity semiconducting (14, 4) carbon nanotubes. ACS Nano, 2017, 11: 186–193
51 Wang J T, Jin X, Liu Z B, et al. Growing highly pure semiconducting carbon nanotubes by electrotwisting the helicity. Nat Catal, 2018, 1: 326–331
52 Hernandez Y, Nicolosi V, Lotya M, et al. High-yield production of graphene by liquid-phase exfoliation of graphite. Nat Nanotech, 2008, 3: 563–568
53 Liu N, Luo F, Wu H X, et al. One-step ionic-liquid-assisted electrochemical synthesis of ionic-liquid-functionalized graphene sheets directly from graphite. Adv Funct Mater, 2008, 18: 1518–1525
54 Kosynkin D V, Higginbotham A L, Sinitskii A, et al. Longitudinal unzipping of carbon nanotubes to form graphene nanoribbons. Nature, 2009, 458: 872–876
55 Jiao L Y, Zhang L, Wang X R, et al. Narrow graphene nanoribbons from carbon nanotubes. Nature, 2009, 458: 877–880
56 Terrones M, Botello-Méndez A R, Campos-Delgado J, et al. Graphene and graphite nanoribbons: morphology, properties, synthesis, defects and applications. Nano Today, 2010, 5: 351–372
57 Yan Q M, Huang B, Yu J, et al. Intrinsic current-voltage characteristics of graphene nanoribbon transistors and effect of edge doping. Nano Lett, 2007, 7: 1469–1473
58 Emtsev K V, Bostwick A, Horn K, et al. Towards wafer-size graphene layers by atmospheric pressure graphitization of silicon carbide. Nat Mater, 2009, 8: 203–207
59 de Heer W A, Berger C, Ruan M, et al. Large area and structured epitaxial graphene produced by confinement controlled sublimation of silicon carbide. Proc Natl Acad Sci USA, 2011, 108: 16900–16905
60 Somani P R, Somani S P, Umeno M. Planer nano-graphenes from camphor by CVD. Chem Phys Lett, 2006, 430: 56–59
61 Li X S, Cai W W, An J, et al. Large-area synthesis of high-quality and uniform graphene films on copper foils. Science, 2009, 324: 1312–1314
62 Lee S, Lee K, Zhong Z H. Wafer scale homogeneous bilayer graphene films by chemical vapor deposition. Nano Lett, 2010, 10: 4702–4707
63 Gao L B, Ren W C, Xu H L, et al. Repeated growth and bubbling transfer of graphene with millimetre-size single-crystal grains using platinum. Nat Commun, 2012, 3: 699
64 Bae S, Kim H, Lee Y, et al. Roll-to-roll production of 30-inch graphene films for transparent electrodes. Nat Nanotech, 2010, 5: 574–578

65 Pei S, Cheng H M. The reduction of graphene oxide. Carbon, 2012, 50: 3210–3228
66 Wang H, Xu X Z, Li J Y, et al. Surface monocrystallization of copper foil for fast growth of large single-crystal graphene under free molecular flow. Adv Mater, 2016, 28: 8968–8974
67 Liu C, Xu X Z, Qiu L, et al. Kinetic modulation of graphene growth by fluorine through spatially confined decomposition of metal fluorides. Nat Chem, 2019, 11: 730–736
68 Xu X Z, Zhang Z H, Dong J C, et al. Ultrafast epitaxial growth of metre-sized single-crystal graphene on industrial Cu foil. Sci Bull, 2017, 62: 1074–1080
69 Yan Z, Peng Z W, Casillas G, et al. Rebar graphene. ACS Nano, 2014, 8: 5061–5068
70 Novaes F D, Rurali R, Ordejón P. Electronic transport between graphene layers covalently connected by carbon nanotubes. ACS Nano, 2010, 4: 7596–7602
71 Varshney V, Patnaik S S, Roy A K, et al. Modeling of thermal transport in pillared-graphene architectures. ACS Nano, 2010, 4: 1153–1161
72 Lin X Y, Liu P, Wei Y, et al. Development of an ultra-thin film comprised of a graphene membrane and carbon nanotube vein support. Nat Commun, 2013, 4: 2920
73 Cohen-Tanugi D, Grossman J C. Water desalination across nanoporous graphene. Nano Lett, 2012, 12: 3602–3608
74 Hong T K, Lee D W, Choi H J, et al. Transparent, flexible conducting hybrid multilayer thin films of multiwalled carbon nanotubes with graphene nanosheets. ACS Nano, 2010, 4: 3861–3868
75 Tristán-López F, Morelos-Gómez A, Vega-Díaz S M, et al. Large area films of alternating graphene-carbon nanotube layers processed in water. ACS Nano, 2013, 7: 10788–10798
76 Fan Z J, Yan J, Zhi L J, et al. A three-dimensional carbon nanotube/graphene sandwich and its application as electrode in supercapacitors. Adv Mater, 2010, 22: 3723–3728
77 Zhu Y, Li L, Zhang C G, et al. A seamless three-dimensional carbon nanotube graphene hybrid material. Nat Commun, 2012, 3: 1225
78 Yu D S, Goh K, Wang H, et al. Scalable synthesis of hierarchically structured carbon nanotube-graphene fibres for capacitive energy storage. Nat Nanotech, 2014, 9: 555–562
79 Ando T, Nakanishi T. Impurity scattering in carbon nanotubes absence of back scattering. J Phys Soc Jpn, 1998, 67: 1704–1713
80 Bolotin K I, Sikes K J, Jiang Z, et al. Ultrahigh electron mobility in suspended graphene. Solid State Commun, 2008, 146: 351–355
81 Gusynin V P, Sharapov S G. Unconventional integer quantum hall effect in graphene. Phys Rev Lett, 2005, 95: 146801
82 Tworzydlo J, Trauzettel B, Titov M, et al. Sub-poissonian shot noise in graphene. Phys Rev Lett, 2006, 96: 246802
83 Ziegler K. Robust transport properties in graphene. Phys Rev Lett, 2006, 97: 266802
84 Han M Y, Özyilmaz B, Zhang Y B, et al. Energy band-gap engineering of graphene nanoribbons. Phys Rev Lett, 2007, 98: 206805
85 Berger C. Electronic confinement and coherence in patterned epitaxial graphene. Science, 2006, 312: 1191–1196
86 Schwierz F. Graphene transistors. Nat Nanotech, 2010, 5: 487–496
87 Geim A K, Novoselov K S. The rise of graphene. Nat Mater, 2007, 6: 183–191
88 Berger C, Song Z M, Li T B, et al. Ultrathin epitaxial graphite: 2D electron gas properties and a route toward graphene-based nanoelectronics. J Phys Chem B, 2004, 108: 19912–19916
89 Lin Y M, Dimitrakopoulos C, Jenkins K A, et al. 100-GHz transistors from wafer-scale epitaxial graphene. Science, 2010, 327: 662–662
90 Wu Y Q, Lin Y M, Bol A A, et al. High-frequency, scaled graphene transistors on diamond-like carbon. Nature, 2011, 472: 74–78
91 Sire C, Ardiaca F, Lepilliet S, et al. Flexible gigahertz transistors derived from solution-based single-layer graphene. Nano Lett, 2012, 12: 1184–1188
92 Kim B J, Lee S K, Kang M S, et al. Coplanar-gate transparent graphene transistors and inverters on plastic. ACS Nano, 2012, 6: 8646–8651
93 Li S L, Miyazaki H, Kumatani A, et al. Low operating bias and matched input-output characteristics in graphene logic inverters. Nano Lett, 2010, 10: 2357–2362
94 Dürkop T, Getty S A, Cobas E, et al. Extraordinary mobility in semiconducting carbon nanotubes. Nano Lett, 2004, 4: 35–39
95 Bachtold A, Hadley P, Nakanishi T, et al. Logic circuits with carbon nanotube transistors. Science, 2001, 294: 1317–1320
96 Sun D M, Timmermans M Y, Tian Y, et al. Flexible high-performance carbon nanotube integrated circuits. Nat Nanotech, 2011, 6: 156–161
97 Sun D M, Timmermans M Y, Kaskela A, et al. Mouldable all-carbon integrated circuits. Nat Commun, 2013, 4: 2302
98 Derycke V, Martel R, Appenzeller J, et al. Carbon nanotube inter- and intramolecular logic gates. Nano Lett, 2001, 1: 453–456
99 Franklin A D, Luisier M, Han S J, et al. Sub-10 nm carbon nanotube transistor. Nano Lett, 2012, 12: 758–762
100 Dong X C, Fu D L, Fang W J, et al. Doping single-layer graphene with aromatic molecules. Small, 2009, 5: 1422–1426
101 Liu Y, Jin Z, Wang J Y, et al. Nitrogen-doped single-walled carbon nanotubes grown on substrates: evidence for framework doping and their enhanced properties. Adv Funct Mater, 2011, 21: 986–992

102 Lv R T, Cui T X, Jun M S, et al. Open-ended, n-doped carbon nanotube-graphene hybrid nanostructures as high-performance catalyst support. Adv Funct Mater, 2011, 21: 999–1006
103 Lin Y M, Appenzeller J, Knoch J, et al. High-performance carbon nanotube field-effect transistor with tunable polarities. IEEE Trans Nanotechnol, 2005, 4: 481–489
104 Yu W J, Kang B R, Lee I H, et al. Majority carrier type conversion with floating gates in carbon nanotube transistors. Adv Mater, 2009, 21: 4821–4824
105 Nosho Y, Ohno Y, Kishimoto S, et al. Relation between conduction property and work function of contact metal in carbon nanotube field-effect transistors. Nanotechnology, 2006, 17: 3412–3415
106 Yamamoto K, Kamimura T, Matsumoto K. Nitrogen doping of single-walled carbon nanotube by using mass-separated low-energy ion beams. Jpn J Appl Phys, 2005, 44: 1611–1614
107 Moriyama N, Ohno Y, Kitamura T, et al. Change in carrier type in high-k gate carbon nanotube field-effect transistors by interface fixed charges. Nanotechnology, 2010, 21: 165201
108 Liu W, Song M S, Kong B, et al. Flexible and stretchable energy storage: recent advances and future perspectives. Adv Mater, 2017, 29: 1603436
109 Khang D Y. A stretchable form of single-crystal silicon for high-performance electronics on rubber substrates. Science, 2006, 311: 208–212
110 Huang J H, Fang J H, Liu C C, et al. Effective work function modulation of graphene/carbon nanotube composite films as transparent cathodes for organic optoelectronics. ACS Nano, 2011, 5: 6262–6271
111 Cao Q, Hur S H, Zhu Z T, et al. Highly bendable, transparent thin-film transistors that use carbon-nanotube-based conductors and semiconductors with elastomeric dielectrics. Adv Mater, 2006, 18: 304–309
112 Aikawa S, Einarsson E, Thurakitseree T, et al. Deformable transparent all-carbon-nanotube transistors. Appl Phys Lett, 2012, 100: 063502
113 Tung V C, Chen L M, Allen M J, et al. Low-temperature solution processing of graphene-carbon nanotube hybrid materials for high-performance transparent conductors. Nano Lett, 2009, 9: 1949–1955
114 Lu R T, Christianson C, Weintrub B, et al. High photoresponse in hybrid graphene-carbon nanotube infrared detectors. ACS Appl Mater Interfaces, 2013, 5: 11703–11707
115 Kim S H, Song W, Jung M W, et al. Carbon nanotube and graphene hybrid thin film for transparent electrodes and field effect transistors. Adv Mater, 2014, 26: 4247–4252
116 Peng L W, Feng Y Y, Lv P, et al. Transparent, conductive, and flexible multiwalled carbon nanotube/graphene hybrid electrodes with two three-dimensional microstructures. J Phys Chem C, 2012, 116: 4970–4978
117 Liu Y J, Liu Y D, Qin S C, et al. Graphene-carbon nanotube hybrid films for high-performance flexible photodetectors. Nano Res, 2017, 10: 1880–1887
118 Liu Y D, Wang F Q, Wang X M, et al. Planar carbon nanotube-graphene hybrid films for high-performance broadband photodetectors. Nat Commun, 2015, 6: 8589
119 Jang S, Jang H, Lee Y, et al. Flexible, transparent single-walled carbon nanotube transistors with graphene electrodes. Nanotechnology, 2010, 21: 425201
120 Liu Y D, Wang F Q, Liu Y J, et al. Charge transfer at carbon nanotube-graphene van der Waals heterojunctions. Nanoscale, 2016, 8: 12883–12886
121 Kholmanov I N, Magnuson C W, Piner R, et al. Optical, electrical, and electromechanical properties of hybrid graphene/carbon nanotube films. Adv Mater, 2015, 27: 3053–3059
122 Yu W J, Lee S Y, Chae S H, et al. Small hysteresis nanocarbon-based integrated circuits on flexible and transparent plastic substrate. Nano Lett, 2011, 11: 1344–1350
123 Yu W J, Chae S H, Lee S Y, et al. Ultra-transparent, flexible single-walled carbon nanotube non-volatile memory device with an oxygen-decorated graphene electrode. Adv Mater, 2011, 23: 1889–1893
124 Jung S, Kim J H, Kim J, et al. Reverse-micelle-induced porous pressure-sensitive rubber for wearable human-machine interfaces. Adv Mater, 2014, 26: 4825–4830
125 Wang X W, Gu Y, Xiong Z P, et al. Silk-molded flexible, ultrasensitive, and highly stable electronic skin for monitoring human physiological signals. Adv Mater, 2014, 26: 1336–1342
126 Park J, Lee Y, Hong J, et al. Giant tunneling piezoresistance of composite elastomers with interlocked microdome arrays for ultrasensitive and multimodal electronic skins. ACS Nano, 2014, 8: 4689–4697
127 Yeom C, Chen K, Kiriya D, et al. Large-area compliant tactile sensors using printed carbon nanotube active-matrix backplanes. Adv Mater, 2015, 27: 1561–1566
128 Zhu B W, Niu Z Q, Wang H, et al. Microstructured graphene arrays for highly sensitive flexible tactile sensors. Small, 2014, 10: 3625–3631
129 Bae G Y, Pak S W, Kim D, et al. Linearly and highly pressure-sensitive electronic skin based on a bioinspired hierarchical structural array. Adv Mater, 2016, 28: 5300–5306
130 Sheng L Z, Liang Y, Jiang L L, et al. Bubble-decorated honeycomb-like graphene film as ultrahigh sensitivity pressure sensors. Adv Funct Mater, 2015, 25: 6545–6551
131 Yao H B, Ge J, Wang C F, et al. A flexible and highly pressure-sensitive graphene-polyurethane sponge based on fractured microstructure design. Adv Mater, 2013, 25: 6692–6698
132 Jian M Q, Xia K L, Wang Q, et al. Flexible and highly sensitive pressure sensors based on bionic hierarchical structures. Adv Funct Mater, 2017, 27: 1606066
133 Li J H, Li W X, Huang W P, et al. Fabrication of highly reinforced and compressible graphene/carbon nanotube hybrid foams via a facile self-assembly process for application as strain sensors and beyond. J Mater Chem C, 2017,

5: 2723–2730
134 Kim K H, Oh Y, Islam M F. Graphene coating makes carbon nanotube aerogels superelastic and resistant to fatigue. Nat Nanotech, 2012, 7: 562–566
135 Sun H Y, Xu Z, Gao C. Multifunctional, ultra-flyweight, synergistically assembled carbon aerogels. Adv Mater, 2013, 25: 2554–2560
136 Li X L, Sha J W, Lee S K, et al. Rivet graphene. ACS Nano, 2016, 10: 7307–7313
137 Nguyen D D, Tai N H, Chen S Y, et al. Controlled growth of carbon nanotube-graphene hybrid materials for flexible and transparent conductors and electron field emitters. Nanoscale, 2012, 4: 632–638
138 Lee D H, Kim J E, Han T H, et al. Versatile carbon hybrid films composed of vertical carbon nanotubes grown on mechanically compliant graphene films. Adv Mater, 2010, 22: 1247–1252
139 Lyth S M, Silva S R P. Field emission from multiwall carbon nanotubes on paper substrates. Appl Phys Lett, 2007, 90: 173124
140 Mani V, Devadas B, Chen S M. Direct electrochemistry of glucose oxidase at electrochemically reduced graphene oxide-multiwalled carbon nanotubes hybrid material modified electrode for glucose biosensor. Biosens Bioelectron, 2013, 41: 309–315
141 Liu F, Piao Y X, Choi K S, et al. Fabrication of free-standing graphene composite films as electrochemical biosensors. Carbon, 2012, 50: 123–133
142 Chen H, Qian W Z, Xie Q, et al. Graphene-carbon nanotube hybrids as robust, rapid, reversible adsorbents for organics. Carbon, 2017, 116: 409–414
143 Gabor N M, Zhong Z H, Bosnick K, et al. Extremely efficient multiple electron-hole pair generation in carbon nanotube photodiodes. Science, 2009, 325: 1367–1371
144 Echtermeyer T J, Britnell L, Jasnos P K, et al. Strong plasmonic enhancement of photovoltage in graphene. Nat Commun, 2011, 2: 458
145 Liu Y, Cheng R, Liao L, et al. Plasmon resonance enhanced multicolour photodetection by graphene. Nat Commun, 2011, 2: 579
146 Lu R T, Shi J J, Baca F J, et al. High performance multiwall carbon nanotube bolometers. J Appl Phys, 2010, 108: 084305
147 He X W, Léonard F, Kono J. Uncooled carbon nanotube photodetectors. Adv Opt Mater, 2015, 3: 989–1011
148 Pei T, Xu H T, Zhang Z Y, et al. Electronic transport in single-walled carbon nanotube/graphene junction. Appl Phys Lett, 2011, 99: 113102
149 Pyo S, Kim W, Jung H I, et al. Heterogeneous integration of carbon-nanotube-graphene for high-performance, flexible, and transparent photodetectors. Small, 2017, 13: 1700918
150 Velten J, Mozer A J, Li D, et al. Carbon nanotube/graphene nanocomposite as efficient counter electrodes in dye-sensitized solar cells. Nanotechnology, 2012, 23: 085201
151 Choi H, Kim H, Hwang S, et al. Dye-sensitized solar cells using graphene-based carbon nano composite as counter electrode. Sol Energy Mater Sol Cells, 2011, 95: 323–325
152 Gan X, Lv R T, Bai J F, et al. Efficient photovoltaic conversion of graphene-carbon nanotube hybrid films grown from solid precursors. 2D Mater, 2015, 2: 034003
153 Chung K, Lee C H, Yi G C. Transferable GaN layers grown on ZnO-coated graphene layers for optoelectronic devices. Science, 2010, 330: 655–657
154 Yoo H, Chung K, Choi Y S, et al. Microstructures of GaN thin films grown on graphene layers. Adv Mater, 2012, 24: 515–518
155 Han N, Cuong T V, Han M, et al. Improved heat dissipation in gallium nitride light-emitting diodes with embedded graphene oxide pattern. Nat Commun, 2013, 4: 1452
156 Lee C H, Kim Y J, Hong Y J, et al. Flexible inorganic nanostructure light-emitting diodes fabricated on graphene films. Adv Mater, 2011, 23: 4614–4619
157 Seo T H, Park A H, Park S, et al. Direct growth of GaN layer on carbon nanotube-graphene hybrid structure and its application for light emitting diodes. Sci Rep, 2015, 5: 7747
158 Qin S C, Wang F Q, Liu Y J, et al. A light-stimulated synaptic device based on graphene hybrid phototransistor. 2D Mater, 2017, 4: 035022
159 Lee M, Lee W, Choi S, et al. Brain-inspired photonic neuromorphic devices using photodynamic amorphous oxide semiconductors and their persistent photoconductivity. Adv Mater, 2017, 29: 1700951
160 Dai S L, Wu X H, Liu D P, et al. Light-stimulated synaptic devices utilizing interfacial effect of organic field-effect transistors. ACS Appl Mater Interfaces, 2018, 10: 21472–21480
161 Qin S C, Chen X Q, Du Q Q, et al. Sensitive and robust ultraviolet photodetector array based on self-assembled graphene/C60 hybrid films. ACS Appl Mater Interfaces, 2018, 10: 38326–38333
162 Qin S C, Jiang H Z, Du Q Q, et al. Planar graphene-C_{60}-graphene heterostructures for sensitive UV-visible photodetection. Carbon, 2019, 146: 486–490
163 Jnawali G, Rao Y, Beck J H, et al. Observation of ground- and excited-state charge transfer at the C_{60}/graphene interface. ACS Nano, 2015, 9: 7175–7185
164 Ojeda-Aristizabal C, Santos E J G, Onishi S, et al. Molecular arrangement and charge transfer in C_{60}/graphene heterostructures. ACS Nano, 2017, 11: 4686–4693
165 Cheng Q, Tang J, Ma J, et al. Graphene and carbon nanotube composite electrodes for supercapacitors with ultra-high energy density. Phys Chem Chem Phys, 2011, 13: 17615

166 Izadi-Najafabadi A, Yasuda S, Kobashi K, et al. Extracting the full potential of single-walled carbon nanotubes as durable supercapacitor electrodes operable at 4 V with high power and energy density. Adv Mater, 2010, 22: E235–E241
167 Zhang D S, Yan T T, Shi L Y, et al. Enhanced capacitive deionization performance of graphene/carbon nanotube composites. J Mater Chem, 2012, 22: 14696
168 Yu D S, Dai L M. Self-assembled graphene/carbon nanotube hybrid films for supercapacitors. J Phys Chem Lett, 2010, 1: 467–470
169 Cheng Q, Tang J, Ma J, et al. Graphene and nanostructured MnO2 composite electrodes for supercapacitors. Carbon, 2011, 49: 2917–2925
170 Yang S Y, Chang K H, Tien H W, et al. Design and tailoring of a hierarchical graphene-carbon nanotube architecture for supercapacitors. J Mater Chem, 2011, 21: 2374–2380
171 Dimitrakakis G K, Tylianakis E, Froudakis G E. Pillared graphene: a new 3-D network nanostructure for enhanced hydrogen storage. Nano Lett, 2008, 8: 3166–3170
172 Mao Y L, Zhong J X. The computational design of junctions by carbon nanotube insertion into a graphene matrix. New J Phys, 2009, 11: 093002
173 Du F, Yu D S, Dai L M, et al. Preparation of tunable 3D pillared carbon nanotube-graphene networks for high-performance capacitance. Chem Mater, 2011, 23: 4810–4816
174 Zhao M Q, Liu X F, Zhang Q, et al. Graphene/single-walled carbon nanotube hybrids: one-step catalytic growth and applications for high-rate Li-S batteries. ACS Nano, 2012, 6: 10759–10769
175 Li S S, Luo Y H, Lv W, et al. Vertically aligned carbon nanotubes grown on graphene paper as electrodes in lithium-ion batteries and dye-sensitized solar cells. Adv Energy Mater, 2011, 1: 486–490
176 Bae S H, Karthikeyan K, Lee Y S, et al. Microwave self-assembly of 3D graphene-carbon nanotube-nickel nanostructure for high capacity anode material in lithium ion battery. Carbon, 2013, 64: 527–536
177 Lv R, Cruz-Silva E, Terrones M. Building complex hybrid carbon architectures by covalent interconnections: graphene-nanotube hybrids and more. ACS Nano, 2014, 8: 4061–4069